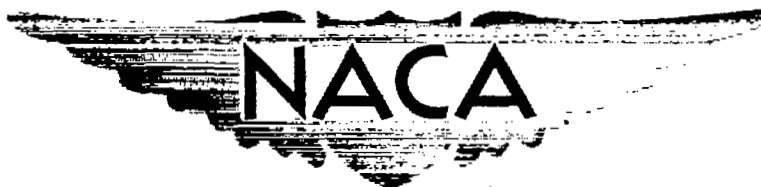UNCLASSIFIED

NACA

RESEARCH MEMORANDUM

CORRELATION OF ANALOG SOLUTIONS WITH EXPERIMENTAL

SEA-LEVEL TRANSIENT DATA FOR CONTROLLED

TURBINE-PROPELLER ENGINE, INCLUDING

ANALOG RESULTS AT ALTITUDES

By James Lazar and Wilfred L. DeRocher, Jr.

Lewis Flight Propulsion Laboratory
Cleveland, Ohio

FOR REFERENCE

CLASSIFICATION CANCELLED

Author: naca R7 2631 Date 9/10/54

NOT TO BE TAKEN FROM THIS ROOM

By mpa 9/24/54

NATIONAL ADVISORY COMMITTEE
FOR AERONAUTICS

WASHINGTON
August 24, 1951

CONFIDENTIAL

UNCLASSIFIED

NATIONAL ADVISORY COMMITTEE FOR AERONAUTICS

RESEARCH MEMORANDUM

CORRELATION OF ANALOG SOLUTIONS WITH EXPERIMENTAL SEA-LEVEL

TRANSIENT DATA FOR CONTROLLED TURBINE-PROPELLER ENGINE

INCLUDING ANALOG RESULTS AT ALTITUDES

By James Lazar and Wilfred L. DeRocher, Jr.

SUMMARY

A satisfactory correlation was obtained between experimental sea-level transient data at constant flight speed and solutions from the analog representation. The analog representation is accomplished by transfer functions that were formed from a frequency-response analysis of the experimental transient data as obtained from the controlled engine. This analog representation was then used to compute system response at altitude.

The engine-control system with an underdamped sea-level turbine-speed response and fixed-control constants resulted in an oscillatory system at 35,000 feet. Variation of control constants to maintain sea-level turbine-speed response at all altitudes resulted in large blade-angle initial overshoot at 35,000 feet. This large blade-angle overshoot may result in over torque at 35,000 feet if the sea-level overshoot approaches maximum allowable torque. Variation of control constants to maintain system loop gain and ratio of engine time constant to control time constant at sea-level values resulted in a similar initial turbine speed and blade-angle overshoots at 35,000 feet, but in an increase in the time required for turbine speed to first reach its final value.

INTRODUCTION

Early flight tests of controlled turbine-propeller engines indicated that a controlled engine system that is stable at low altitudes and low flight speeds is not necessarily stable at high altitudes and high flight speeds (reference 1). In collaboration with the Air Materiel Command, U. S. Air Force, an investigation was initiated at the NACA Lewis laboratory to study reasons for the trend toward instability with increase in altitude and flight speed, to provide a means for predicting the altitude behavior on a controlled turbine-propeller engine, and to indicate means for avoiding instability at altitude or high flight speed.

In order to accomplish the objectives of this program, the Air
Materiel Command provided the NACA with turbine-propeller engines and
several types of control system. The first phase of this engine
investigation showed that the dynamic relation of turbine speed to
fuel flow or blade angle is approximately a first-order lag and that
linear differential equations are applicable over the sea-level
static operating range of the T31-1 turbine-propeller engine
(reference 2).

This report presents the correlation of analog solutions with
experimental sea-level transient data for the Aeroproducts AT-1
(modified) control on the T31-1 engine and analog results for alti-
tude conditions at zero ram. The control varies blade angle to
obtain a desired turbine speed while the power output of the engine
is varied by adjusting the engine fuel flow. The control is essen-
tially integral plus proportional in action and was modified by the
manufacturer at the request of the NACA so that the amount of
integral and the amount of proportional action could be varied.

Transient-response data for the engine and the control were
obtained from operation of the controlled engine system in a sea-
level static test stand. A transfer-function representation of each
of the loop components was determined from analysis of the transient
data. These component transfer functions were used to represent the
system on an analog and because the comparison of analog solutions
and experimental data was satisfactory, the transfer functions were
used to study the altitude response of the system. The analog repre-
sentation was first used to investigate the effect of altitude on the
controlled engine system with fixed control constants. In addition,
two methods of varying the control constants to compensate for the
effect of altitude on the system were studied.

APPARATUS AND INSTRUMENTATION

Engine

Type	Turbine propeller, T31-1
Compressor	Axial flow
Burner section	Nine reverse-flow combustion chambers
Turbine	Single stage, mixed flow
Exhaust nozzle	Fixed area
Speed range	11,000 to 13,000 rpm
Maximum turbine-outlet temperature	1265° F

Propeller

Type	Aeroproducts A542F-17
Diameter	12 feet, 1 inch
Beta arm	Input lever for propeller-pitch-change mechanism
Action	Proportional relation between beta arm and blade angle
Pitch-change mechanism	Hydraulic, self contained

Control

Type	Aeroproducts AT-1 (modified)
Action	Proportional plus integral
Control mechanism	Hydraulic, self contained
Modifications	Proportional and integral constants were provided with range of adjustments by Aeroproducts Division of General Motors Corporation

Steady-State Instruments

Turbine speed	a-c. tachometer generator coupled to drag-type tachometer indicator; maximum error $\pm1/3$ of 1 percent for full scale
Engine fuel flow	Calibrated A.S.M.E. sharp-edged orifice with bellows-type differential pressure gage; maximum error ±1 percent of full scale
Propeller-blade angle	Position circuit (fig. 1); maximum error $\pm1/2^{\circ}$
Speed-setting-lever position	Position circuit (fig. 1); maximum error ±1 percent of full scale
Load torque	Oil pressure of self-balancing hydraulic system, which acts on ring gear in reduction unit; maximum error ±1 percent of full scale
Turbine-outlet temperature	Chromel-alumel thermocouple; maximum error $\pm20^{\circ}$ F

2114

Transient Instruments

Turbine speed	d-c. tachometer generator with filter circuit to oscillograph galvanometer; break frequency of filter circuit, 0.53 cycle per second
Engine fuel flow	Position circuit (fig. 1); potentiometer connected to pointer of differential pressure gage connected to A.S.M.E. sharp-edged orifice; natural frequency, 10 to 15 cycles per second
Propeller-blade angle	Position circuit (fig. 1); potentiometer connected to blade shank; slip-ring device used for electrical connection; natural frequency of oscillograph element, 40 cycles per second
Speed-setting-lever position	Position circuit (fig. 1); natural frequency of oscillograph element, 40 cycles per second
Propeller-input-lever (beta arm) position	Position circuit (fig. 1); natural frequency of oscillograph element, 40-cycles-per-second
Turbine-outlet temperature	Chromel-alumel thermocouple; break frequency, 0.1 cycle per second
Transient-data recorder	Photorecording oscillograph with critically damped 40-cycles-per-second galvanometer elements (changes recorded from initial operating point). Each oscillogram was calibrated by photographs of steady-state instruments taken before and after each run.
Time scale	10 cycles per second; voltage from audio-oscillator. Checked by 60 cycles-per-second line frequency.

DETERMINATION OF TRANSFER FUNCTIONS

For purposes of analysis, the engine and the control system are
represented by the block diagram of figure 2. All symbols are defined
in the appendix. Each of the system components, control, propeller-
pitch-change mechanism, engine, and speed-measuring instrument, are
indicated by a block. In each of the blocks, the transfer

function KG(iω) relates the output to the input of that particular
block (reference 3). Speed error is formed by a comparison of
required speed and measured speed. The power output of the engine is
varied by the engine fuel flow.

The determination of the transfer function for each component
of the control system was necessary for the analog studies. Three
steps were used to determine the transfer functions: obtaining con-
trolled engine experimental transient-response data, harmonic anal-
ysis and frequency-response calculations, and fitting the transfer
functions to the frequency-response data.

Transient response of controlled system to disturbances in
speed setting. - It was desired to determine the transfer functions
of speed to blade angle, blade angle to beta arm, and beta arm to
speed error. Transient changes in turbine speed, blade angle, beta
arm, and speed setting were recorded on a photorecording oscillograph
for ramp-type disturbances in speed setting. The engine fuel flow
was maintained constant throughout these runs. These transient data
were obtained for various values of the integral and proportional
control constants,which could be varied independently by two screw-
type adjustments. An example of a transient run is shown in
figure 3, which includes the 10-cycle-per-second timing marks.
Contact with successive turns on the winding of the potentiometers
created the multitude of small steps in the traces of speed setting,
blade angle, and beta arm. The temperature trace is not sufficiently
accurate to be useful because of the low sensitivity.

Harmonic analysis and frequency response. - In order to deter-
mine the transfer function of each system component (fig. 2), the
frequency characteristic of each component was formed. The trans-
formation from the time domain to the frequency domain was accom-
plished by harmonic analysis. Methods of harmonic analysis that are
used in this report and that apply to gas-turbine engines are dis-
cussed in reference 4. For this particular work, the integrals of
the harmonic analysis were evaluated using Bickley's approximation
formula for six differences with an IBM digital computer.

Results of the harmonic analysis of the input and output to each
component are combined to compute the frequency characteristic. The
frequency characteristic may be represented by the amplitude ratio
and the phase angle of the output with respect to the input of the
component as a function of frequency. The phase angle and the log-
arithm of the amplitude ratio were plotted against the logarithm
of the frequency for each of the components,as is shown in figure 4.

Frequency-response data for the engine and the speed-measuring instrument are shown in figures 4(a) and 4(b), for the propeller-pitch-change mechanism in figures 4(c) and 4(d), and for the control in figures 4(e) and 4(f). Figure 4 is discussed in greater detail in the next section.

Transfer functions of system components. - A transfer function may be considered as a function of frequency and thus a frequency characteristic can be prepared for each transfer function. Conversely, each frequency characteristic may be represented by a transfer function.

For the engine and the speed-measuring instrument, the frequency characteristic as defined by the data points in figures 4(a) and 4(b) indicates that the transfer function may be two lags in series. The form of the transfer function is

$$\left[KG(i\omega)\right]_e \left[KG(i\omega)\right]_r = \left(\frac{-K_e}{1+i\tau_e\omega}\right)\left(\frac{K_r}{1+i\tau_r\omega}\right) \tag{1}$$

From equation (1), the amplitude ratio A and the phase angle Φ written as functions of frequency ω are

$$A = K_e K_r \sqrt{\left(\frac{1}{1+\tau_e^2\omega^2}\right)\left(\frac{1}{1+\tau_r^2\omega^2}\right)} \tag{2}$$

and

$$\Phi = \tan^{-1}\frac{-\omega(\tau_e+\tau_r)}{1-\tau_e\tau_r\omega^2} \tag{3}$$

Equation (3) may be written for values of ω at $-45°$ and at $-90°$ from figure 4(b) and the two simultaneous equations solved for engine and speed-measuring time constants, τ_e and τ_r, respectively. The value of speed-measuring-instrument gain K_r is 1 so that the steady-state value of the measured turbine speed N_m is the actual turbine speed N_e. The engine gain K_e is the ratio of the steady-state change in turbine speed to the steady-state change in blade angle β. The negative sign before K_e in equation (1) is the result of an increase in speed due to a decrease in blade angle. Equations (2) and (3) with appropriate values of the constants have been plotted as the dashed lines in figures 4(a) and 4(b), respectively. For frequencies less than 2 radians per second, the variation between the experimental frequency characteristic and the transfer-function

2114

approximation is in the order of 2 percent in the amplitude ratio
against frequency plot (fig. 4(a)) and in the order of 4° in the
phase angle against frequency plot (fig. 4(b)). Reference 2 and
more recent data indicate that the transfer function of turbine
speed to blade angle is a first-order lag, thus the second lag is
attributed to the speed-measuring instrument.

The action of the propeller-pitch-change mechanism is such
that a position of the input (beta arm) results in a corresponding
position of the output (blade angle). An examination of transient
data indicated that the propeller-pitch-change mechanism had a dead
band and also a lag due to the hydraulic amplifier. The dead-band
effect can be observed in figure 3 where the blade angle does not
move until the beta arm has arrived at some value. As these non-
linearities are not easily represented, a first-order lag

$\left[KG(i\omega)\right]_\beta = \dfrac{K_\beta}{1+i\tau_\beta\omega}$ was assumed to represent the transfer function

for the propeller-pitch-change mechanism. The variation in time
constant for a series of runs was determined using the 22.5° point
on the plot of phase angle against frequency. The time constant
fell in the range of 0.2 to 0.45 second with 0.3 second as an
average. The propeller-pitch-change-mechanism gain K_β was made
unity so that the units could all be combined in the proportional
and integral constants of the control. The frequency characteristic
of the propeller-pitch-change-mechanism transfer function approxima-
tion $\left[KG(i\omega)\right]_\beta = \dfrac{1}{1+i\ 0.3\ \omega}$ is plotted as the dashed lines of

figures 4(c) and 4(d). For frequencies less than 2 radians per
second, the variation between the transfer-function approximation
and the frequency characteristic is of the order of 20 percent for
the amplitude ratio against frequency plot in figure 4(c) and of
the order of 6° for the phase angle against frequency plot of
figure 4(d).

The data points in figures 4(e) and 4(f) define the frequency
characteristic of the control and indicate that the form of the
control transfer function should be integral plus proportional,
that is,

$$\left[KG(i\omega)\right]_c = -\left(K_p+\frac{K_i}{i\omega}\right) = -K_p\left(1+\frac{1}{i\tau_c\omega}\right) \tag{4}$$

where the control time constant τ_c is equal to control proportional
constant K_p divided by control integral constant K_i. From equa-
tion (4), the amplitude ratio and phase angle are

$$A = \sqrt{K_p^2 + \frac{K_i^2}{\omega^2}} \tag{5}$$

and

$$\Phi = \tan^{-1} \frac{K_i}{K_p \omega} \tag{6}$$

The amplitude ratio approaches K_p as ω approaches infinity.
The value of K_p is taken as the value of the amplitude ratio at the
higher frequencies of figure 4(e). Scale factors for the amplitude
ratio are determined from the calibration of the experimental transient
runs. Also from equation (5), the amplitude ratio is approximately
equal to K_i/ω for low values of frequency. For a value of K_p
determined from the high frequencies in figure 4(e) and a value of K_i
determined from the low frequencies in figure 4(e), the resulting fre-
quency characteristic of the transfer function did not agree too well
with the experimental frequency characteristic as defined by the data
points in figures 4(e) and 4(f). An examination of the accuracy of
the method used to compute the experimental frequency characteristic
of figures 4(e) and 4(f) indicated that inaccuracies were more prob-
able in the low-frequency range. These inaccuracies are due to the
fact that a small error in either speed setting or turbine speed,
when these quantities are approximately equal, means a large error
in their difference. Because of this inaccuracy, the dotted lines
of figures 4(e) and 4(f) were obtained by substituting other values
of K_i into equations (5) and (6) until a reasonable approximation
was found. For frequencies less than 2 radians per second, the
variation between the transfer-function approximation and the exper-
imental frequency characteristic is of the order of 20 percent for
the amplitude ratio against frequency plot in figure 4(e) and of
the order of 14° for the phase angle against frequency plot in
figure 4(f).

Range of control constants. - It is possible to adjust inde-
pendently the values of the integral and proportional constants for
the control by two screw-type adjustments. The proportional setting
is defined as the number of turns of the adjusting screw from its
full-out position and the integral setting is defined as the number

of turns of the adjusting screw from its full-in position. Several
runs were made at each setting of the control adjusting screws. The
results of these runs are presented in the control calibration curves
(figs. 5(a) and 5(b)). The proportional constant may be varied from
approximately 0.004° to 0.0085° per rpm and the integral constant
from approximately 0.0025° to 0.0061° per second per rpm. For any
position of the control adjusting screws, the values of the propor-
tional and integral constants may vary as much as 15 percent from
the values as given by curves in figure 5. This error is due in
part to a steady-state instrumentation error of ±10 percent of the
transient change and in part to an inability to measure the actual
input (speed error) to the control.

COMPARISON OF ANALOG SOLUTIONS WITH EXPERIMENTAL DATA

The transfer functions were used as a basis to form an analog
of the system. Analog solutions were obtained for comparison with
experimental transient data to determine the validity of the repre-
sentation.

An electronic-type analog was used in this study. The analog
block diagram is similar to the control-system block diagram presented
in figure 2. Scale factors were determined from the criterion that
loop gains for the real and analog systems be identical. The max-
imum time for the analog to complete a solution determined the time
scale factor. Analog solutions are displayed in the form of traces
on a cathode-ray oscilloscope with time as the abscissa and a system
parameter as the ordinate.

A comparison of computed and experimental transient response
data is shown in figure 6. For the experimental transient data
(figs. 6(a) and 6(b)), the control constants were set close to
their maximum values and for the experimental transient data
(figs. 6(c) and 6(d)), the setting was close to minimum values.
The transfer functions and their constants for the analog solutions
of figure 6 were determined by the preceding method from the
experimental transient data. In all cases, the number of oscilla-
tions and the percentage overshoot of the analog solutions and the
experimental transient data were similar. The deviation of the
analog solutions from the experimental data is partly due to the
nonlinearities of the propeller-pitch-change mechanism. One of
these nonlinearities is indicated in the photorecording oscillo-
graph trace of figure 3 as the time elapsed from the initial beta-
arm movement to the initial blade-angle movement. If the analog

solutions are translated to the right by the amount of this elapsed time, about 0.3 second, a much better agreement between the analog solutions and the experimental transient data will be obtained.

As the agreement between the analog solutions and experimental transient data is considered to be satisfactory, an analog investigation of response at altitude could be made.

ALTITUDE RESPONSE OF CONTROLLED SYSTEM

For the engine, there are two factors that vary with altitude under conditions of constant flight speed: (1) the engine gain factor, and (2) the engine time constant. The engine time constant has been shown analytically to vary with altitude pressure and temperature (reference 5) in accordance with the following relation:

$$\tau_e = \tau_{e,corr} \frac{\sqrt{\theta}}{\delta}$$

where τ_e is the engine time constant for any altitude, $\tau_{e,corr}$ is the time constant for NACA standard sea-level conditions, θ is the temperature ratio, and δ is the pressure correction factor. This relation has also been experimentally verified at this laboratory. Correction factors are also applied to the engine gain as follows

$$K_{e,corr} = \frac{\Delta N_{corr}}{\Delta\beta_{corr}} = \frac{\Delta N}{\sqrt{\theta}} \cdot \frac{1}{\Delta\beta} = \frac{K_e}{\sqrt{\theta}}$$

or

$$K_e = K_{e,corr} \sqrt{\theta}$$

where K_e is the engine gain at any altitude and $K_{e,corr}$ is the engine gain at NACA standard sea-level conditions. Based on NACA standard altitude tables, the variation in engine time constant from sea level to 35,000 feet is 371 percent of its sea-level value, whereas the variation in engine gain factor from sea level to 35,000 feet is only 13 percent.

For analog studies, a single sea-level value of engine time constant was considered. This requires an examination of the values of the engine time constant throughout the sea-level operating range of the engine. Sea-level equilibrium characteristics

of the T31-1 engine with the Aeroproducts A542F-17 propeller are
shown in figure 7 where load torque, referred to the turbine, is
plotted against turbine speed for lines of constant blade angle
and for lines of constant fuel flow. The acute angle between the
intersection of a line of constant fuel flow and a line of constant
blade angle has been shown to be indicative of the engine time con-
stant (reference 2). It can be seen that variation of this angle is
less than two to one; thus the variation of the engine time constant
will also be in the order of two to one. As the variation in engine
time constant is not large, a representative value of 2.9 seconds was
chosen and a single study performed for this operating point.
Another factor is that fuel-flow disturbances are not considered in
the analog studies because the stability of a linear system may be
studied by means of either fuel flow or speed-setting disturbances.
In this report, only speed-setting disturbances were investigated.

Altitude pressure and temperature were not sensed by the
original control component, thus the control constants do not vary
with altitude. In order to investigate the condition of control
constants invariant with altitude, analog solutions for turbine-
speed and blade-angle response were obtained for sea level,
25,000 feet, and 35,000 feet.

The system response was also investigated for two methods of
control compensation at 35,000 feet. These two methods of control
compensation are: (1) control constants varied to maintain the
sea-level turbine-speed response at all altitudes, and (2) control
constants varied to maintain the sea-level loop gain and the ratio
of engine time constant to control time constant at all altitudes.

Control constants invariant with altitude. - The control con-
stants were not designed to vary with altitude or flight speed, thus
the system response was investigated for the condition of fixed
control constants assuming constant flight speed. For this condi-
tion, only the engine gain factor and engine time constant vary
with altitude. The values of the component constants and the
response of turbine speed and blade angle to a sudden change in
speed setting for the three altitudes are shown in figures 8(a)
and 8(b). The system becomes more oscillatory as the altitude
is increased as shown in figure 8(a), and the initial turbine-
speed overshoot at 35,000 feet is twice the initial overshoot
at sea level. In addition, as the altitude increases from sea
level to 35,000 feet, the time for turbine speed to initially
reach its final value increases from 1 second to 3.5 seconds and
the time for turbine speed to settle out at its final value
increases from 12 seconds to 65 seconds. The blade-angle response
curves of figure 8(b) show the same forms of oscillation as the

speed response curves; also, the initial overshoot at 35,000 feet is approximately twice the initial overshoot at sea level. Variation in the final value of blade angle is due to the change in the engine gain factor with altitude. It should be noted that the effect of variation in flight speed is not considered in this report.

An engine and control system, if operated as shown by the turbine-speed and blade-angle responses of figures 8(a) and 8(b) for 35,000 feet, could be seriously damaged, particularly when operated near the speed limit. Thus, this system with an underdamped sea-level turbine-speed response and fixed control constants may result in an unsafe system at 35,000 feet. If the control constants had been chosen to give a slightly under-damped system at 35,000 feet and were invariant with altitude, then an overdamped system with a very long time to reach its final value would result at sea level.

Control constants varied to maintain sea-level turbine-speed response at all altitudes. - One of the primary difficulties with the system when the control constants were fixed was the widely varing speed response with altitude under conditions of constant flight velocity. Because of this variation in speed response with fixed control constants, an investigation was conducted to determine the values of control constants that would result in sea-level turbine-speed response at 35,000 feet. The values of loop constants and the turbine-speed and blade-angle responses for 35,000 feet are shown in figures 9(a) and 9(b) as curve 2. Turbine-speed response as shown by curve 2 (fig. 9(a)) is identical to the sea-level turbine-speed response, curve 1. However, the blade-angle response as shown by curve 2 is very different from the sea-level blade-angle response, curve 1 (fig. 9(b)). The blade-angle initial overshoot is 650 percent of final blade-angle change and the blade-angle initial undershoot is 100 percent of final blade-angle change at 35,000 feet. These high values of blade-angle overshoot and undershoot could result in excessive torques and possible damage to the reduction gearing. At increased altitudes, however, an increase in blade-angle overshoot over that at sea level can be tolerated because of altitude density reductions.

The advantage of this system is the identical speed response at all altitudes. The disadvantages are the excessive blade-angle initial overshoot and initial undershoot at high altitude and the complication of additional sensing and computing equipment in the control to attain the altitude compensation.

Control constant varied to maintain sea-level loop gain and ratio of engine time constant to control time constant at all altitudes. - Another method of altitude compensation investigated was the condition of fixed loop gain and fixed ratio of engine time constant to control

time constant. In general, if the loop gain and the time con-
stant ratio are fixed, then the response will be similar at all
altitudes. However, at an altitude of 35,000 feet, the propeller-
pitch-change-mechanism lag and the turbine-speed-recording lag become
insignificant with respect to the increased engine and control time
constants, and the response is less oscillatory at 35,000 feet than at
sea level. The values of the loop constants and the turbine-speed and
blade-angle responses for 35,000 feet are shown in figures 9(a) and 9(b)
as curve 3.

The initial overshoot of the speed response at 35,000 feet as
shown by curve 3 is less than the initial overshoot of the speed
response at sea level, as shown by curve 1 (fig. 9(a)). However, the
time for turbine speed to initially reach its final value at
35,000 feet is about 3 seconds as compared to only about 1 second at
sea level. The initial blade-angle overshoot at 35,000 feet is 110 per-
cent of the final blade-angle change as shown by curve 3 and 140 percent
at sea level, curve 1 (fig. 9(b)). The disadvantages are the increasing
rise time from sea level to 35,000 feet and the need for altitude
sensing and computing equipment. A faster rise time may be achieved at
35,000 feet if a more oscillatory system can be tolerated at sea level.

SUMMARY OF RESULTS

An analog representation of a turbine-propeller engine and control
system was formulated from sea-level static experimental transient
data. A satisfactory correlation was obtained between analog solutions
and the experimental transient data. The analog representation was
used to compute system response at altitude from which the following
conclusions may be drawn:

1. The actual engine-control system with an underdamped turbine-
speed response at sea level and fixed control constants resulted in
twice the initial turbine-speed overshoot at 35,000 feet as at sea-
level and the time for turbine speed to settle out at its final value
increased from approximately 12 seconds at sea level to about
65 seconds at 35,000 feet.

2. Variation of control constants to maintain sea-level turbine-
speed response at all altitudes resulted in the initial blade-angle
overshoot increasing from 140 percent of final blade-angle change at
sea level to 650 percent at 35,000 feet.

3. Variation of control constants to maintain system loop gain
and ratio of engine time constant to control time constant at sea-level

values resulted in similar initial turbine-speed and blade-angle over-shoots at all altitudes, but an increase in the time required for turbine speed to first reach its final value from 1 second at sea level to 3 seconds at 35,000 feet. However, if a more oscillatory system may be tolerated at 35,000 feet, this method may be modified to provide a faster rise time at 35,000 feet.

Lewis Flight Propulsion Laboratory,
     National Advisory Committee for Aeronautics,
          Cleveland, Ohio,

APPENDIX - SYMBOLS

A amplitude ratio, $|KG(i\omega)|$

$[KG(i\omega)]_c$ control transfer function

$[KG(i\omega)]_e$ engine transfer function

$[KG(i\omega)]_r$ speed-measuring-instrument transfer function

$[KG(i\omega)]_\beta$ propeller-pitch-change-mechanism transfer function

$G(i\omega)$ function of $i\omega$ representing time dependent part of transfer function

K constant or frequency invariant portion of transfer function

K_e engine gain, rpm/deg β

K_i control integral constant, $\dfrac{\text{deg } \beta/\text{sec}}{\text{rpm}}$

K_p control proportional constant, deg β/rpm

K_r speed-measuring-instrument gain, rpm/rpm

K_β propeller-pitch-change-mechanism gain, deg β/deg β

N_e actual turbine speed, rpm

N_m measured turbine speed, rpm

N_s turbine-speed setting, rpm

Q load torque referred to turbine, ft-lb

W_f fuel flow, lb/hr

i imaginary number, $i^2 = -1$

β propeller-blade angle, deg

β_a propeller beta arm, deg

θ temperature correction factor,
$$\frac{\text{ambient static temperature}}{\text{NACA standard sea-level temperature}}$$

δ pressure correction factor,
$$\frac{\text{ambient static pressure}}{\text{NACA standard sea-level pressure}}$$

ϕ phase angle, $\tan^{-1}\dfrac{\text{imaginary part of } KG(i\omega)}{\text{real part of } KG(i\omega)}$

τ_c control time constant, sec

τ_e engine time constant, sec

τ_r speed-measuring time constant, sec

τ_β propeller-pitch-change-mechanism time constant, sec

ω frequency, radians/sec

Subscripts:

corr   altitude corrected value

REFERENCES

1. Davis, Frank W.: Problems of Gas-Turbine-Propeller Combinations. Aero. Eng. Rev., vol. 7, no. 4, April 1948, pp. 30-36.

2. Taylor, Burt L., III, and Oppenheimer, Frank L.: Investigation of Frequency-Response Characteristics of Engine Speed for a Typical Turbine-Propeller Engine. NACA TN 2184, 1950.

3. Brown, Gordon S., and Campbell, Donald P.: Principles of Servomechanisms. John Wiley & Sons, Inc., 1948.

4. LaVerne, Melvin E., and Boksenbom, Aaron S.: Frequency Response of Linear Systems from Transient Data. NACA Rep. 977, 1950. (Formerly NACA TN 1935.)

5. Otto, Edward W., and Taylor, Burt L., III: Dynamics of a Turbojet Engine Considered as a Quasi-Static System. NACA TN 2091, 1950.
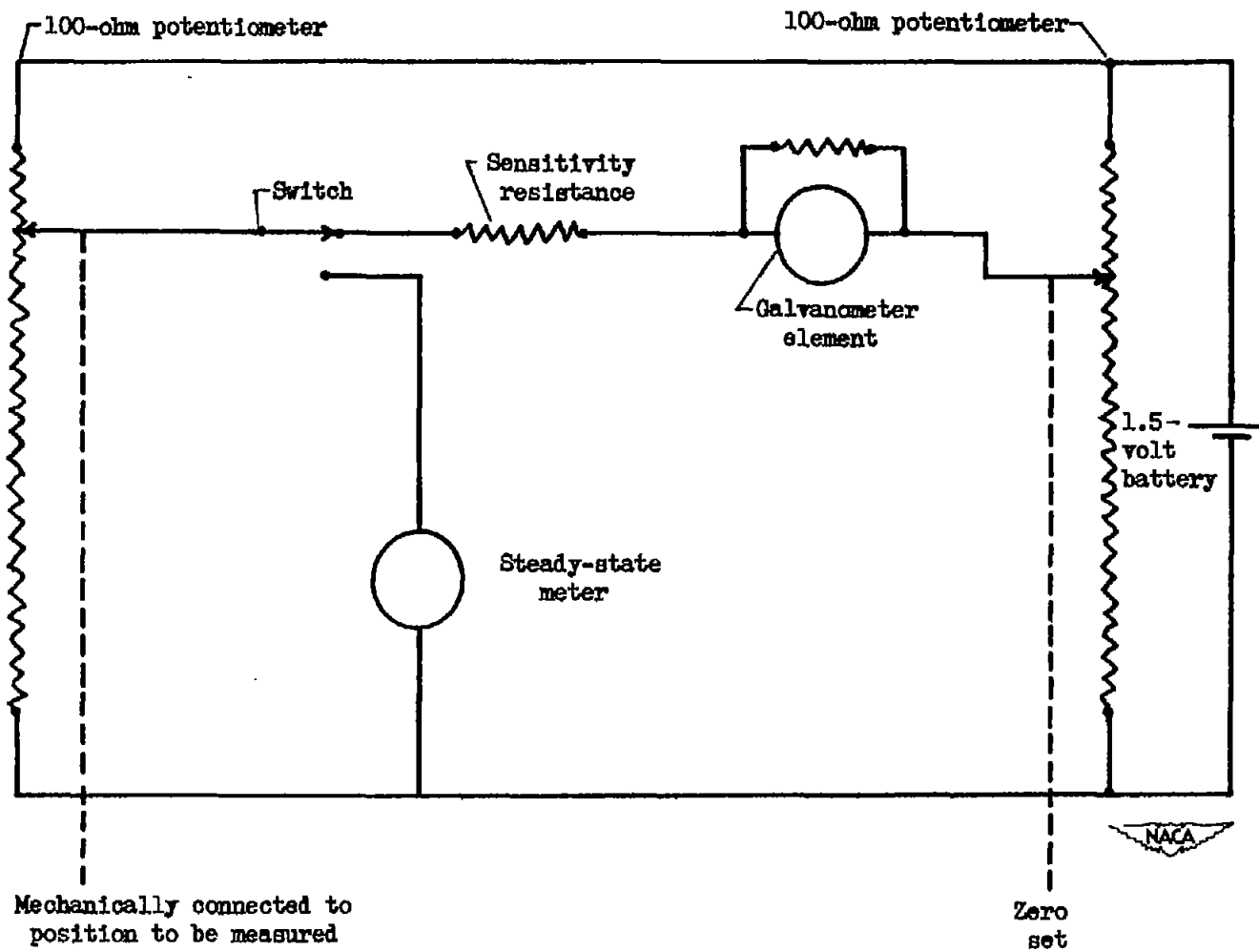
Figure 1. - Schematic diagram of typical steady-state and transient position measuring circuit.
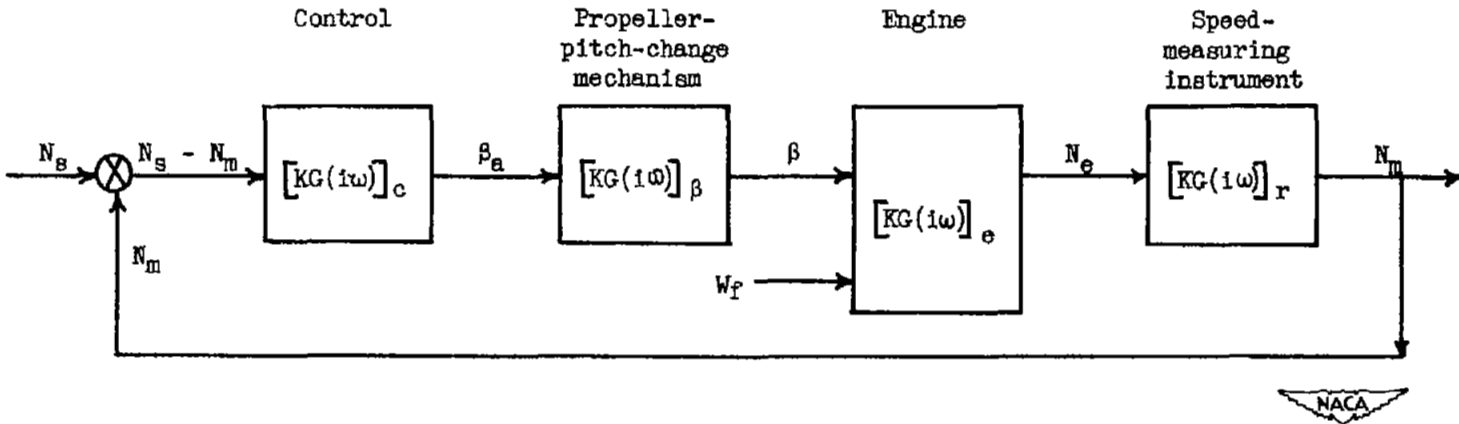
Control   Propeller-pitch-change mechanism   Engine   Speed-measuring instrument

$$N_s \quad \xrightarrow{N_s - N_m} \quad \left[KG(i\omega)\right]_c \quad \xrightarrow{\beta_a} \quad \left[KG(i\omega)\right]_\beta \quad \xrightarrow{\beta} \quad \left[KG(i\omega)\right]_e \quad \xrightarrow{N_e} \quad \left[KG(i\omega)\right]_r \quad \xrightarrow{N_m}$$

N_m

$W_f \longrightarrow$

NACA

Figure 2. - Block diagram of turbine-speed - blade-angle control on turbine-propeller engine for analysis and analog studies.
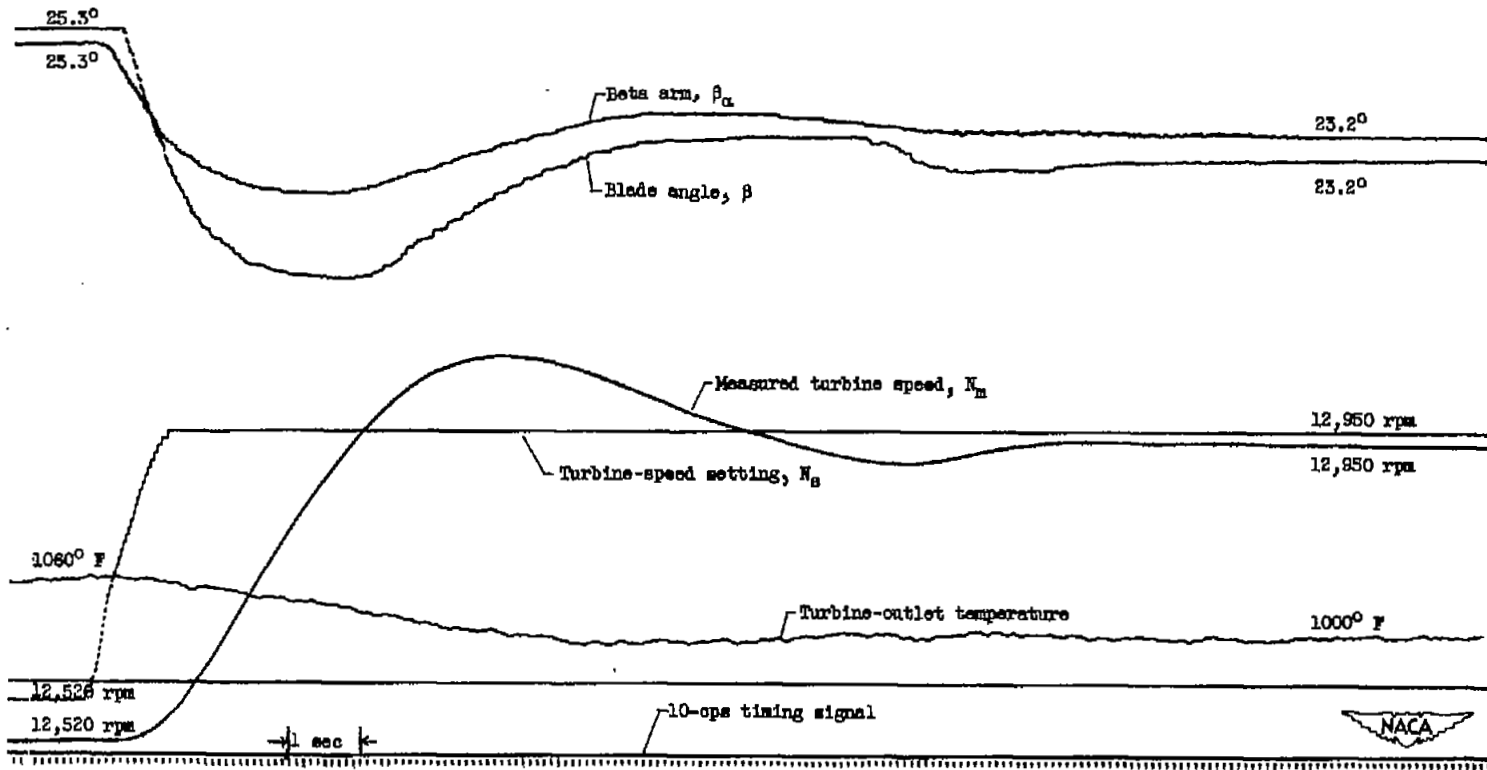
Figure 3. - Typical transient recording showing system responses to ramp-type disturbance in speed setting with constant fuel flow for turbine-propeller engine and turbine-speed - blade-angle control system.
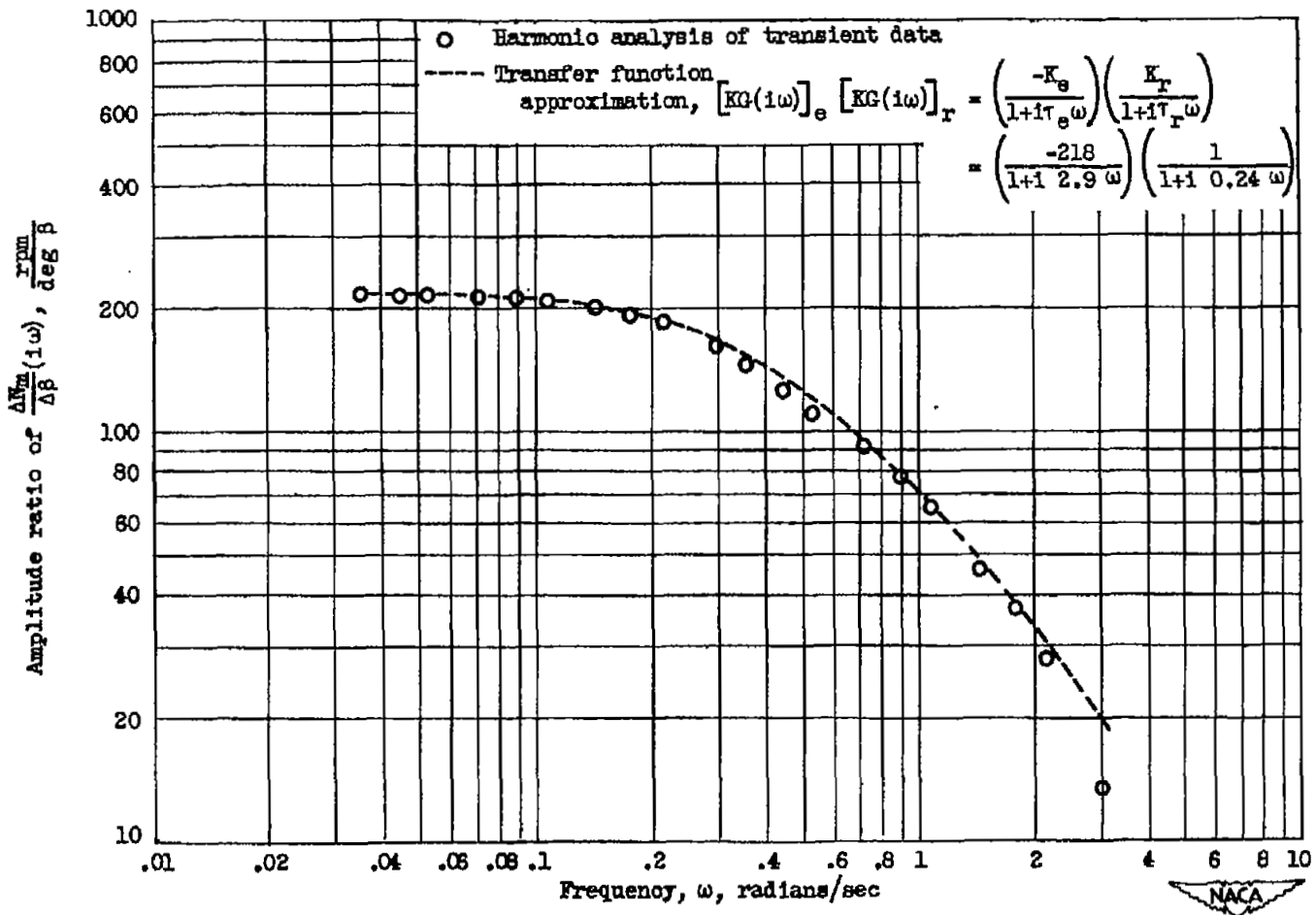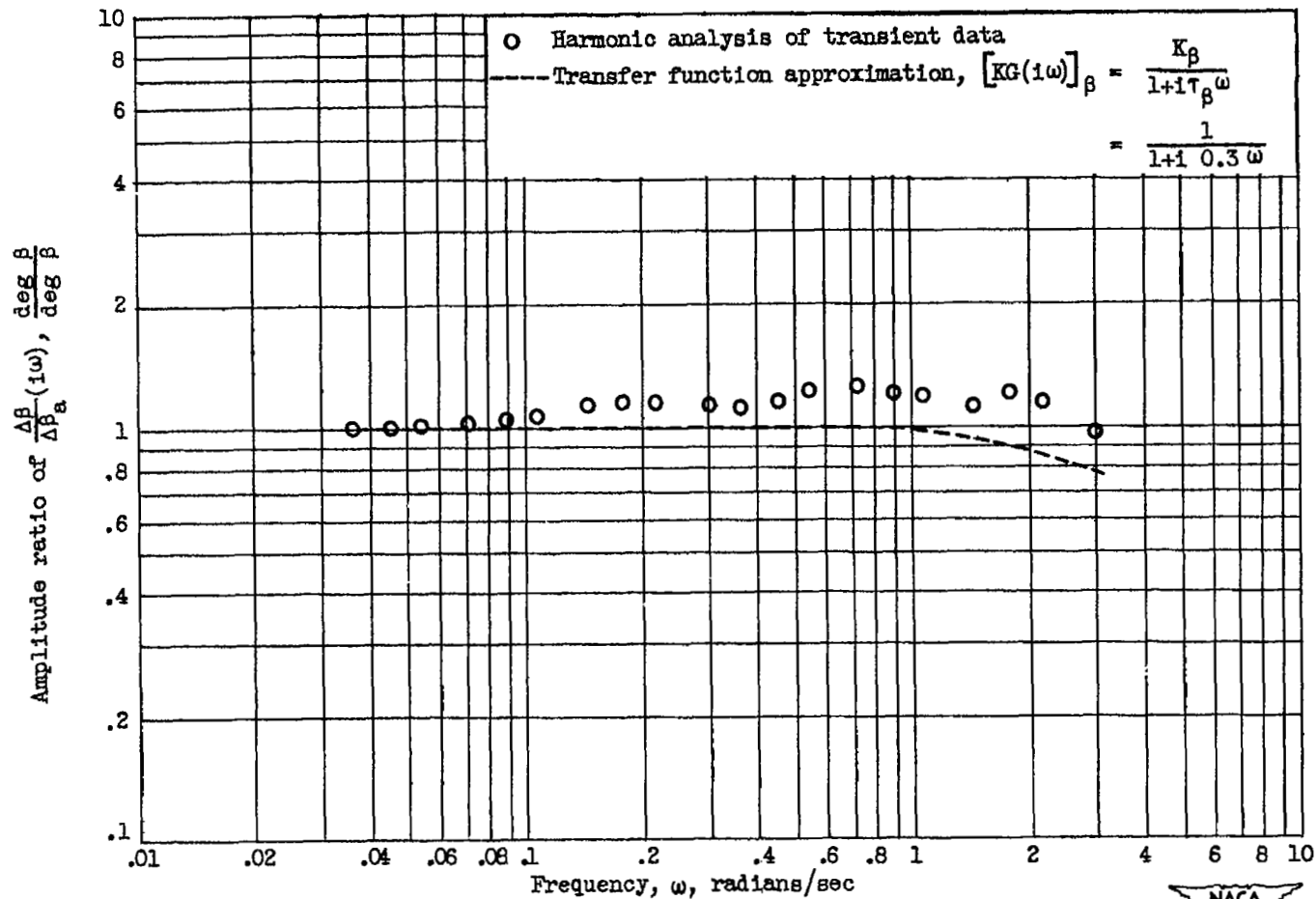
(a) Engine and speed-measuring instrument amplitude ratio relation.

Figure 4. - Frequency characteristic of system components as determined from harmonic analysis of experimental transient response to ramp-type disturbances in speed setting with constant fuel flow and as approximated by transfer functions for turbine-propeller engine and turbine-speed - blade-angle control system.
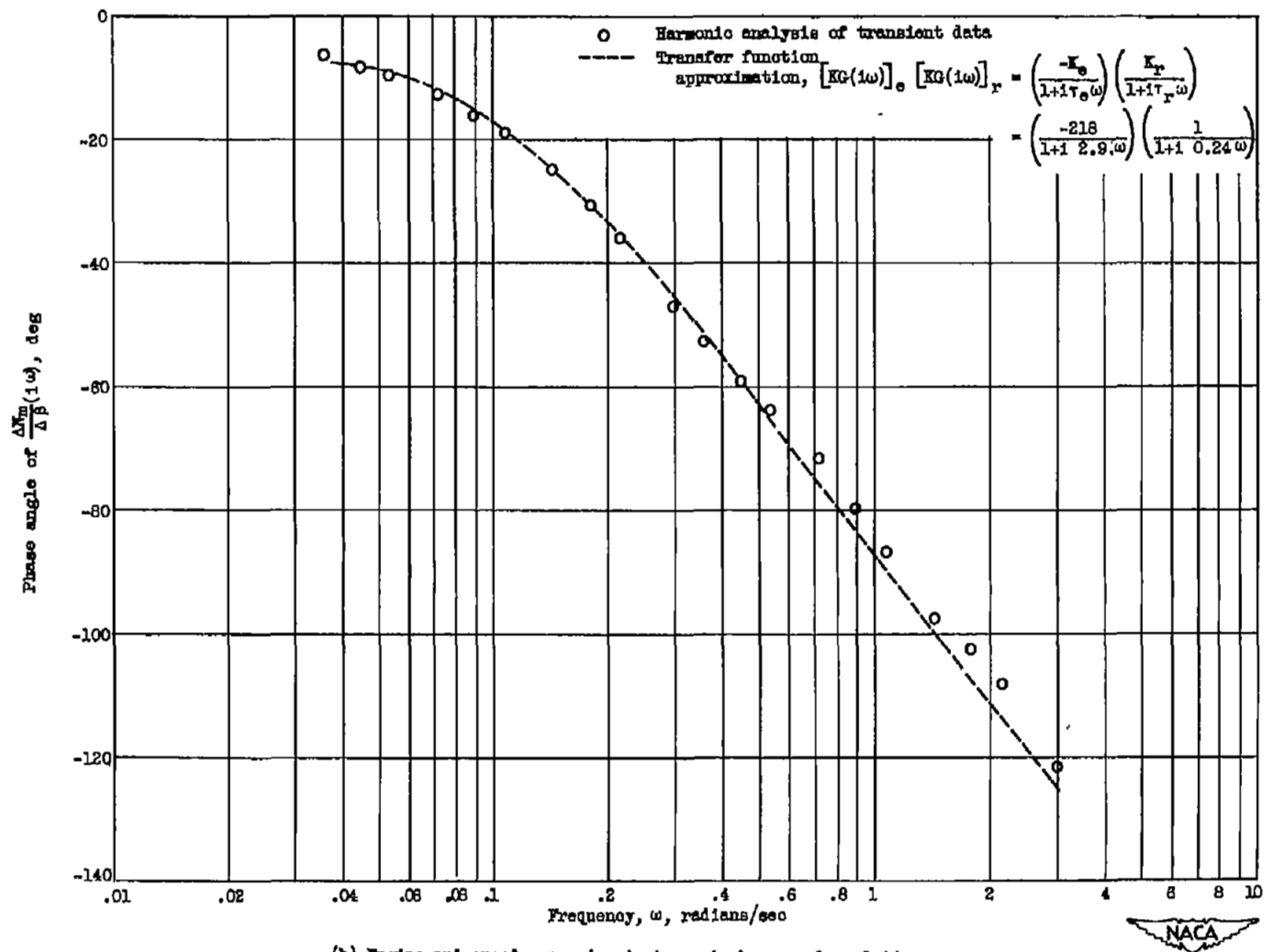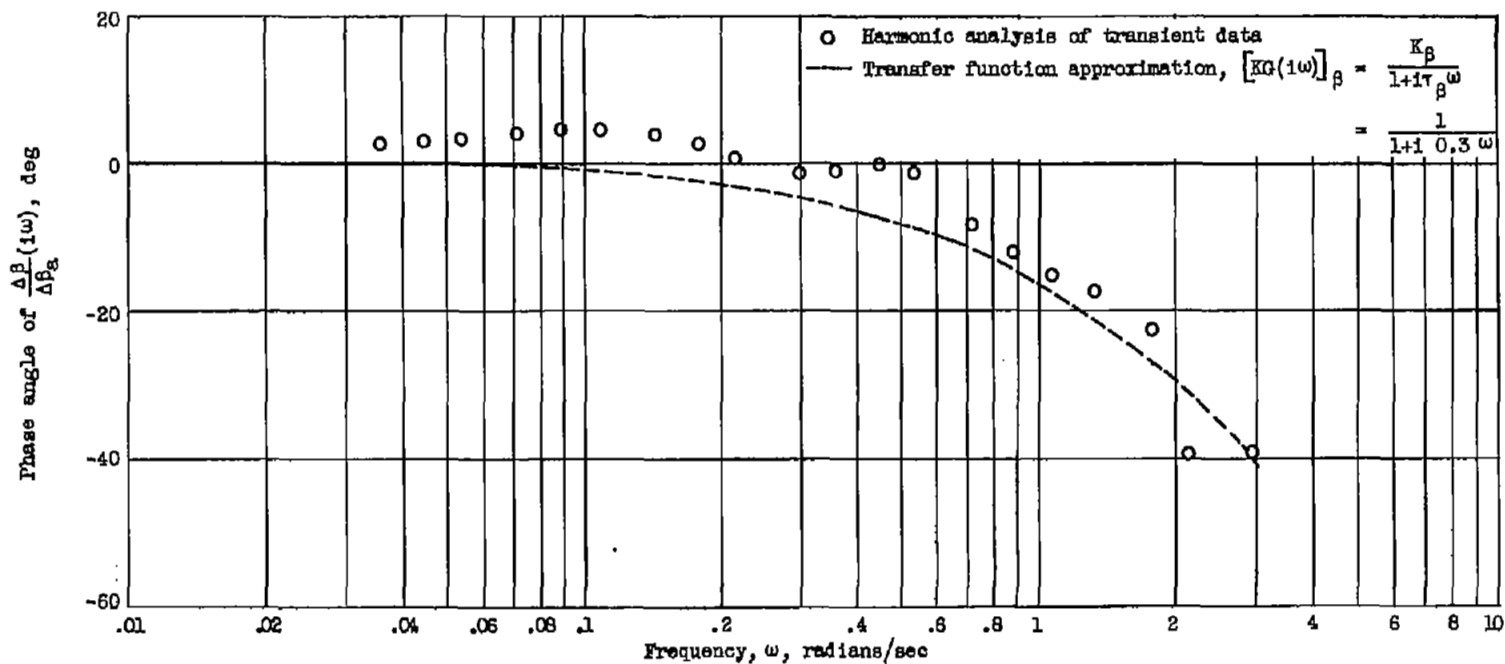
(b) Engine and speed-measuring instrument phase angle relation.

Figure 4. - Continued. Frequency characteristic of system components as determined from harmonic analysis of experimental transient response to ramp-type disturbances in speed setting with constant fuel flow and as approximated by transfer functions for turbine-propeller engine and turbine-speed - blade-angle control system.

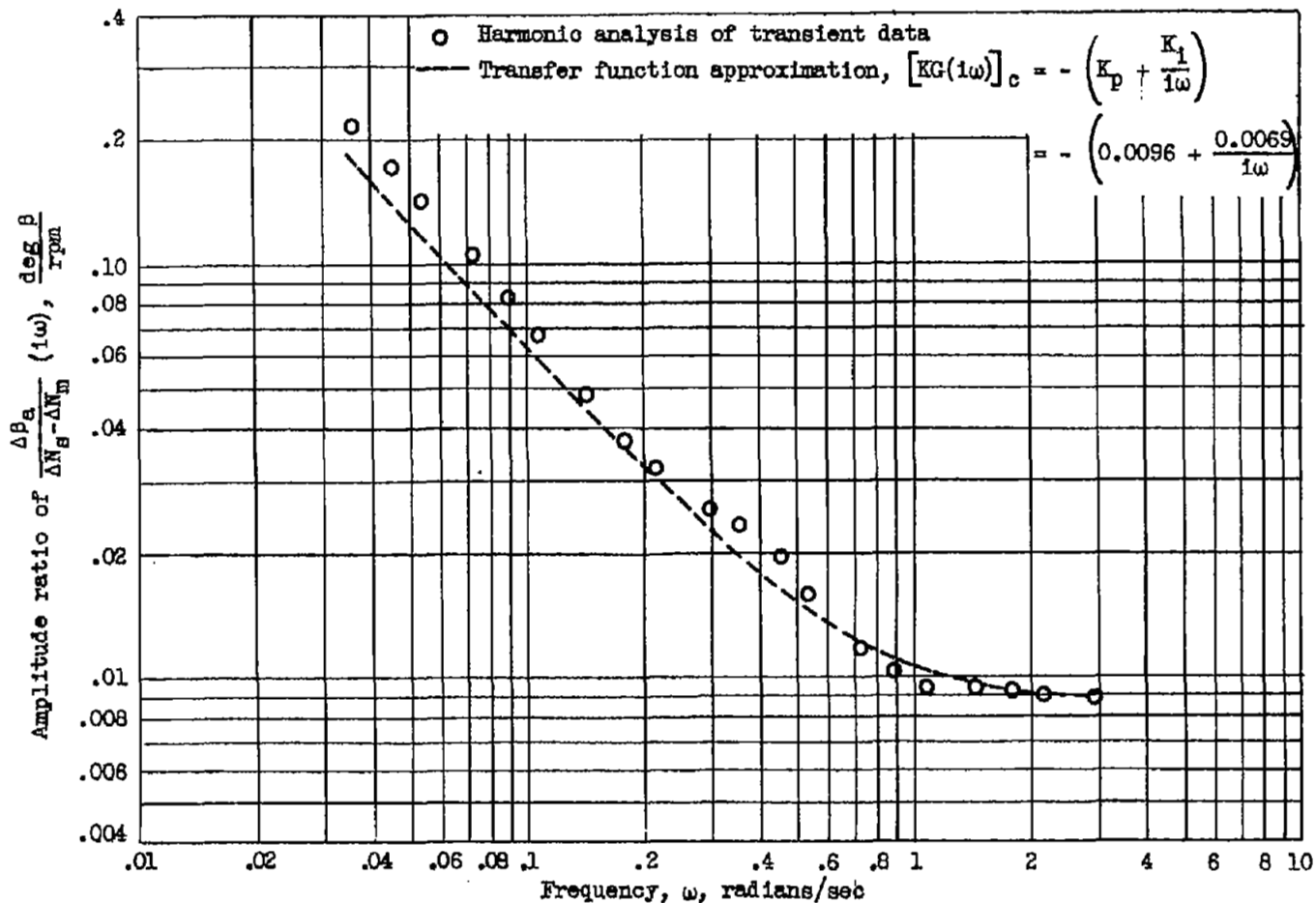(c) Propeller-pitch-change mechanism amplitude ratio relation.

Figure 4. - Continued. Frequency characteristic of system components as determined from harmonic analysis of experimental transient response to ramp-type disturbances in speed setting with constant fuel flow and as approximated by transfer functions for turbine-propeller engine and turbine-speed - blade-angle control system.

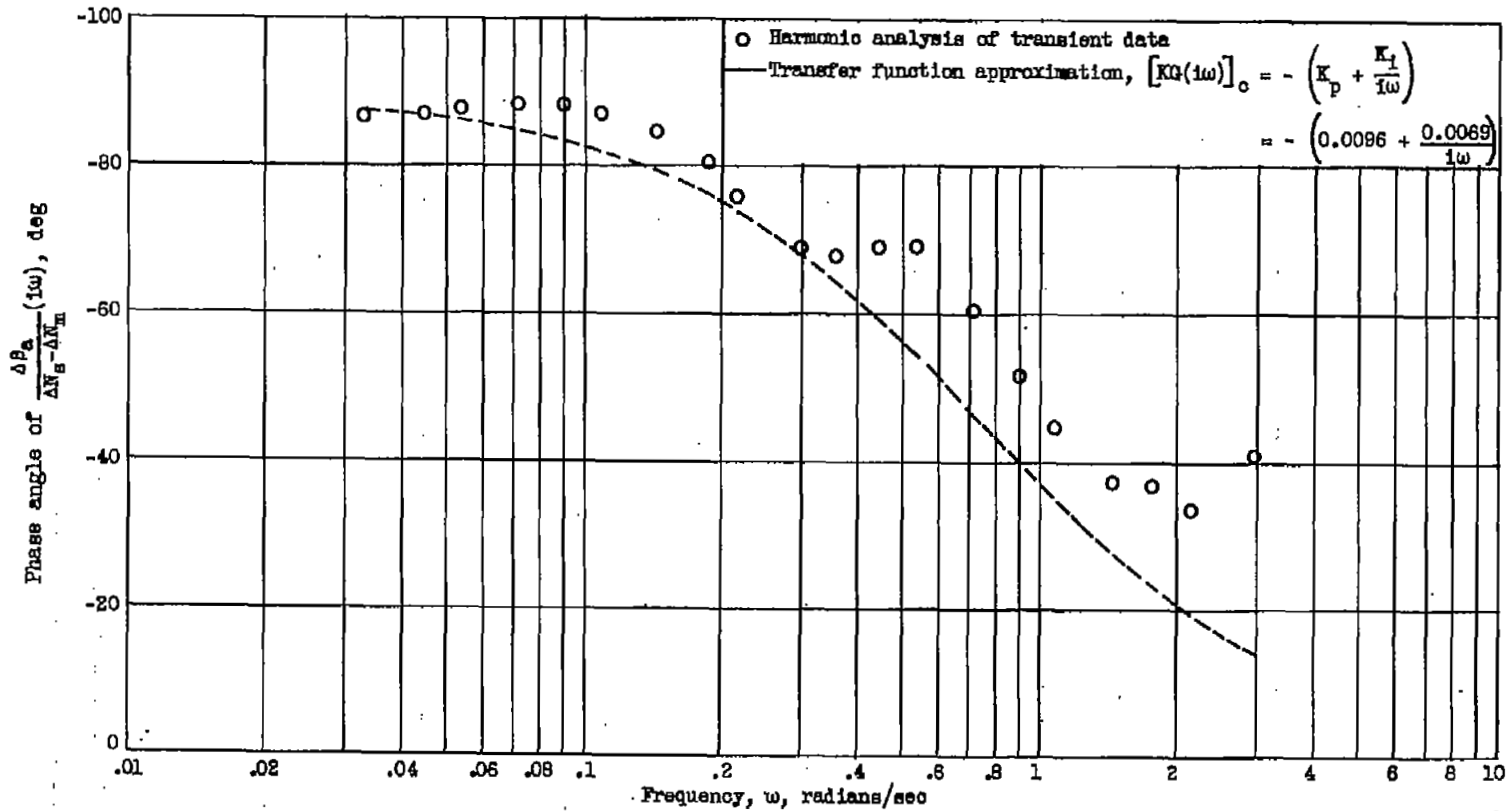(d) Propeller-pitch-change mechanism phase angle relation.

Figure 4. - Continued. Frequency characteristic of system components as determined from harmonic analysis of experimental transient response to ramp-type disturbances in speed setting with constant fuel flow and as approximated by transfer functions for turbine-propeller engine and turbine-speed - blade-angle control system.

(e) Control amplitude ratio relation.

Figure 4. - Continued. Frequency characteristic of system components as determined from harmonic analysis of experimental transient response to ramp-type disturbances in speed setting with constant fuel flow and as approximated by transfer functions for turbine-propeller engine and turbine-speed - blade-angle control system.

(f) Control phase angle relation.

Figure 4. — Concluded. Frequency characteristic of system components as determined from harmonic analysis of experimental transient response to ramp-type disturbances in speed setting with constant fuel flow and as approximated by transfer functions for turbine-propeller engine and turbine-speed - blade-angle control system.
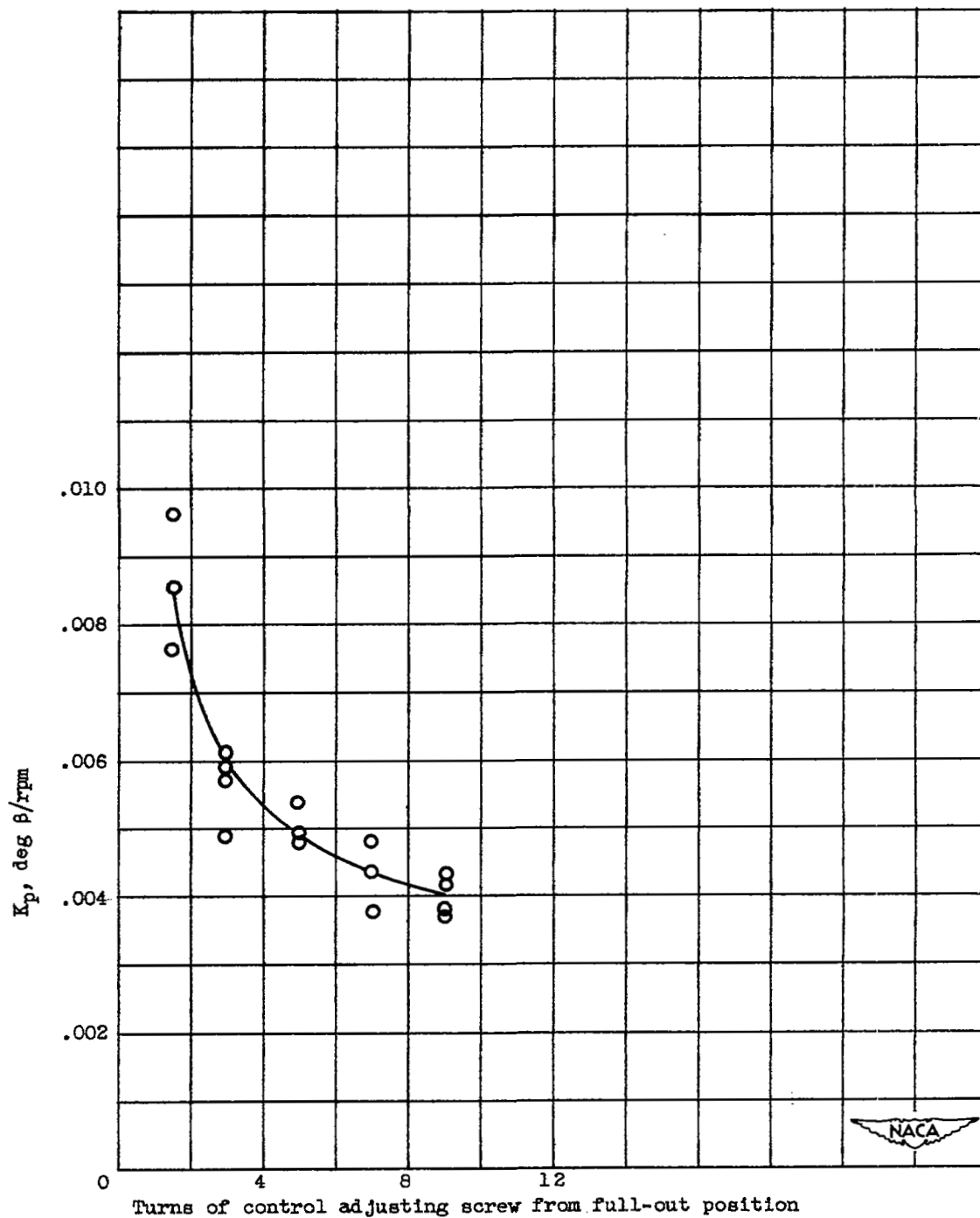
(a) Proportional constant K_p.

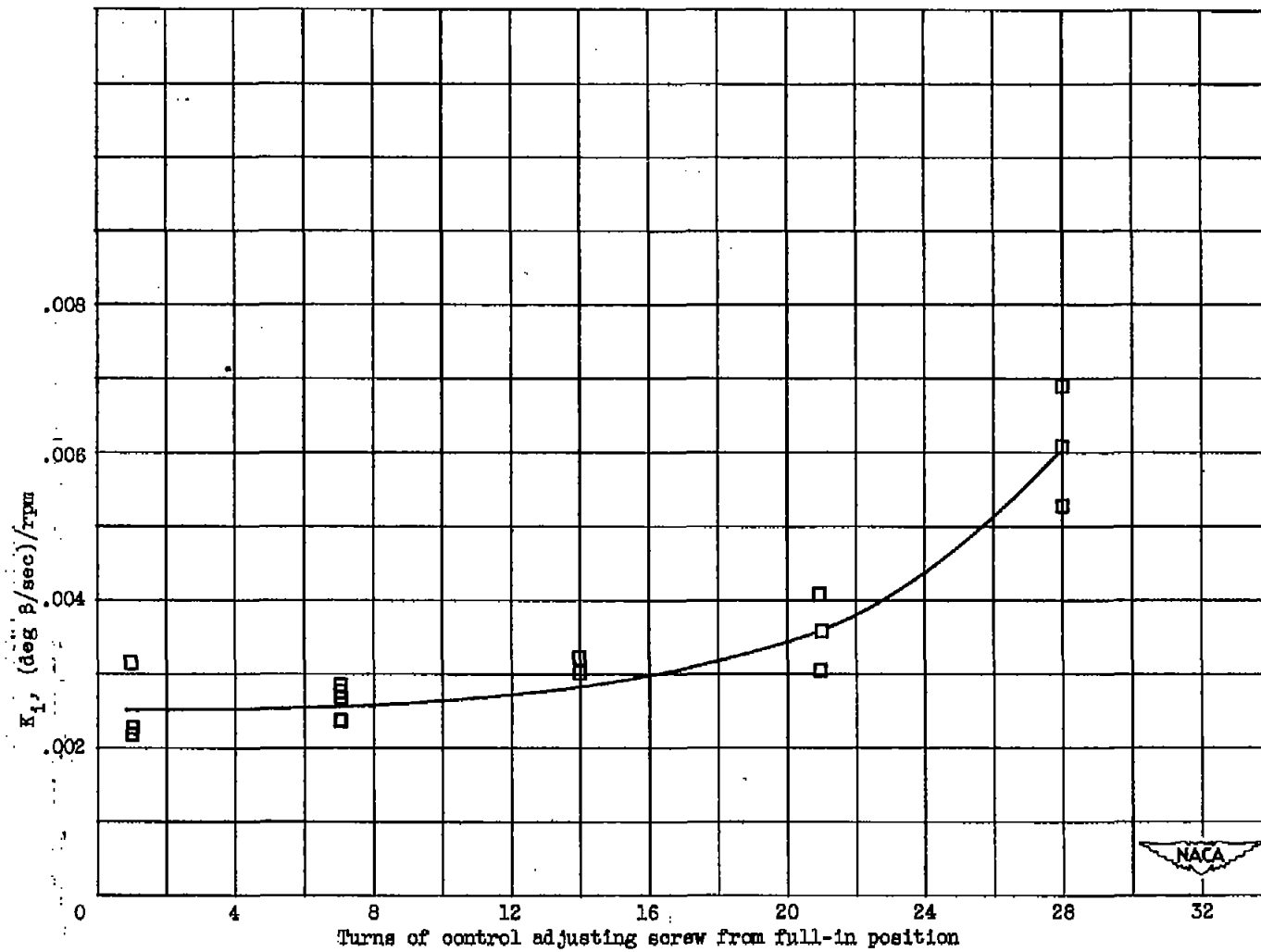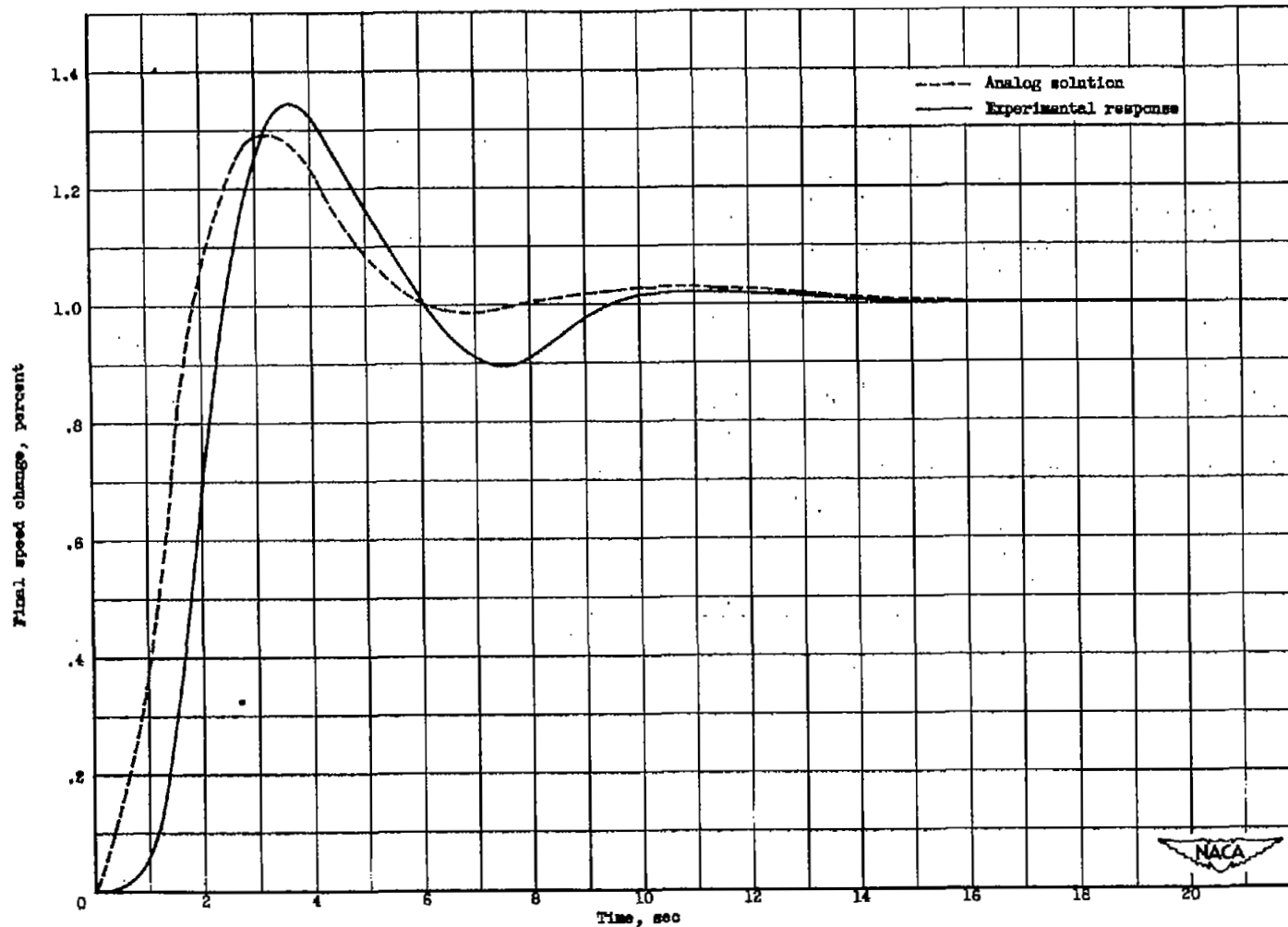Figure 5. - Calibration of turbine-speed - blade-angle control.

(b) Integral constant K_1.

Figure 5. - Concluded. Calibration of turbine-speed - blade-angle control.

(a) Turbine speed. K_p, 0.0084 deg β/rpm; K_i, 0.0068 (deg β/sec)/rpm; $τ_o$, 1.23 sec; turbine-speed change, 11,940 to 12,410 rpm; blade-angle change, 30.3° to 28.1°; load-torque change, 504 to 465 foot-pounds.

Figure 6. – Comparison of experimental transient response and analog solutions to ramp-type disturbances in speed setting with constant fuel flow for turbine-propeller engine and turbine-speed - blade-angle control system. (Analog solution determined from harmonic analysis and transfer function approximation.)
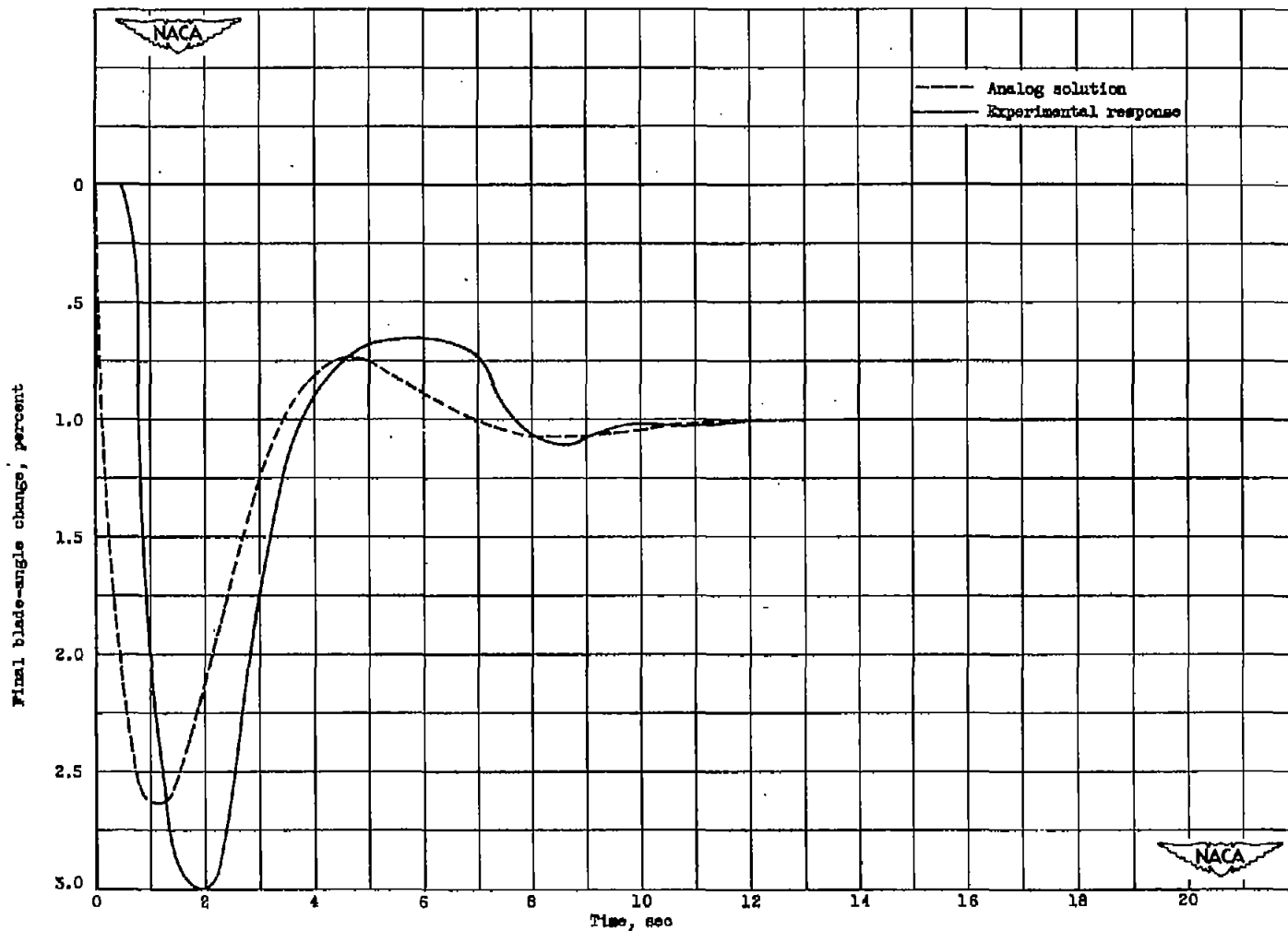
(b) Blade angle. K_p, 0.0084 deg β/rpm; K_i, 0.0068 (deg β/sec)/rpm; τ_0, 1.23 sec; turbine-speed change, 11,940 to 12,410 rpm; blade-angle change, 30.3° to 28.1°; load-torque change, 504 to 485 foot-pounds.

Figure 6. - Continued. Comparison of experimental transient response and analog solutions to ramp-type disturbances in speed setting with constant fuel flow for turbine-propeller engine and turbine-speed - blade-angle control system. (Analog solution determined from harmonic analysis and transfer function approximation.)
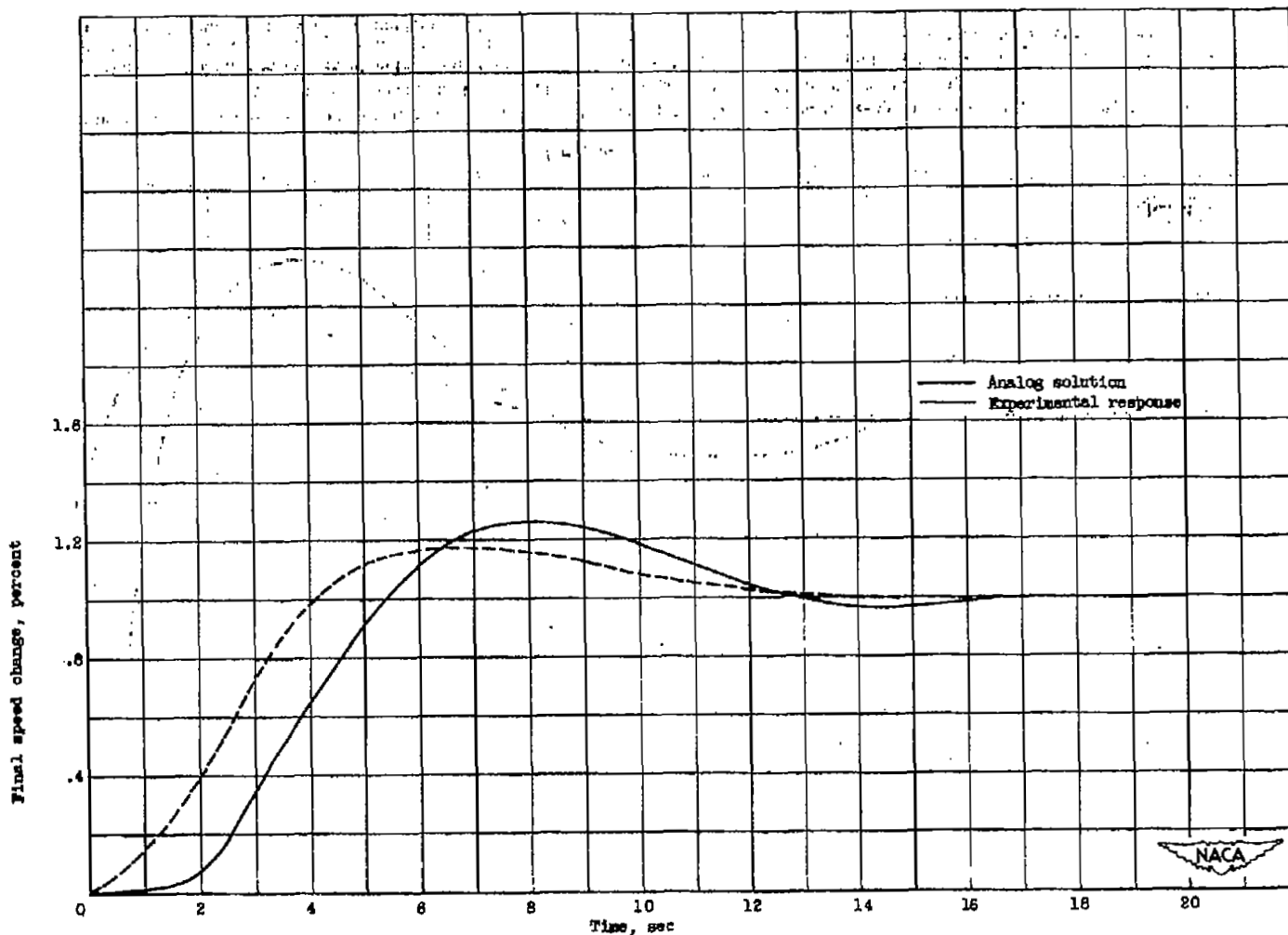
(c) Turbine speed. K_p, 0.0040 deg β/rpm; K_1, 0.0052 (deg β/sec)/rpm; τ_0, 1.25 sec; turbine-speed change, 11,440 to 12,080 rpm; blade-angle change, 26.4° to 23.4°; load-torque change, 333 to 279 foot-pounds.

Figure 6. - Continued. Comparison of experimental transient response and analog solutions to ramp-type disturbances in speed setting with constant fuel flow for turbine-propeller engine and turbine-speed - blade-angle control system. (Analog solution determined from harmonic analysis and transfer function approximation.)
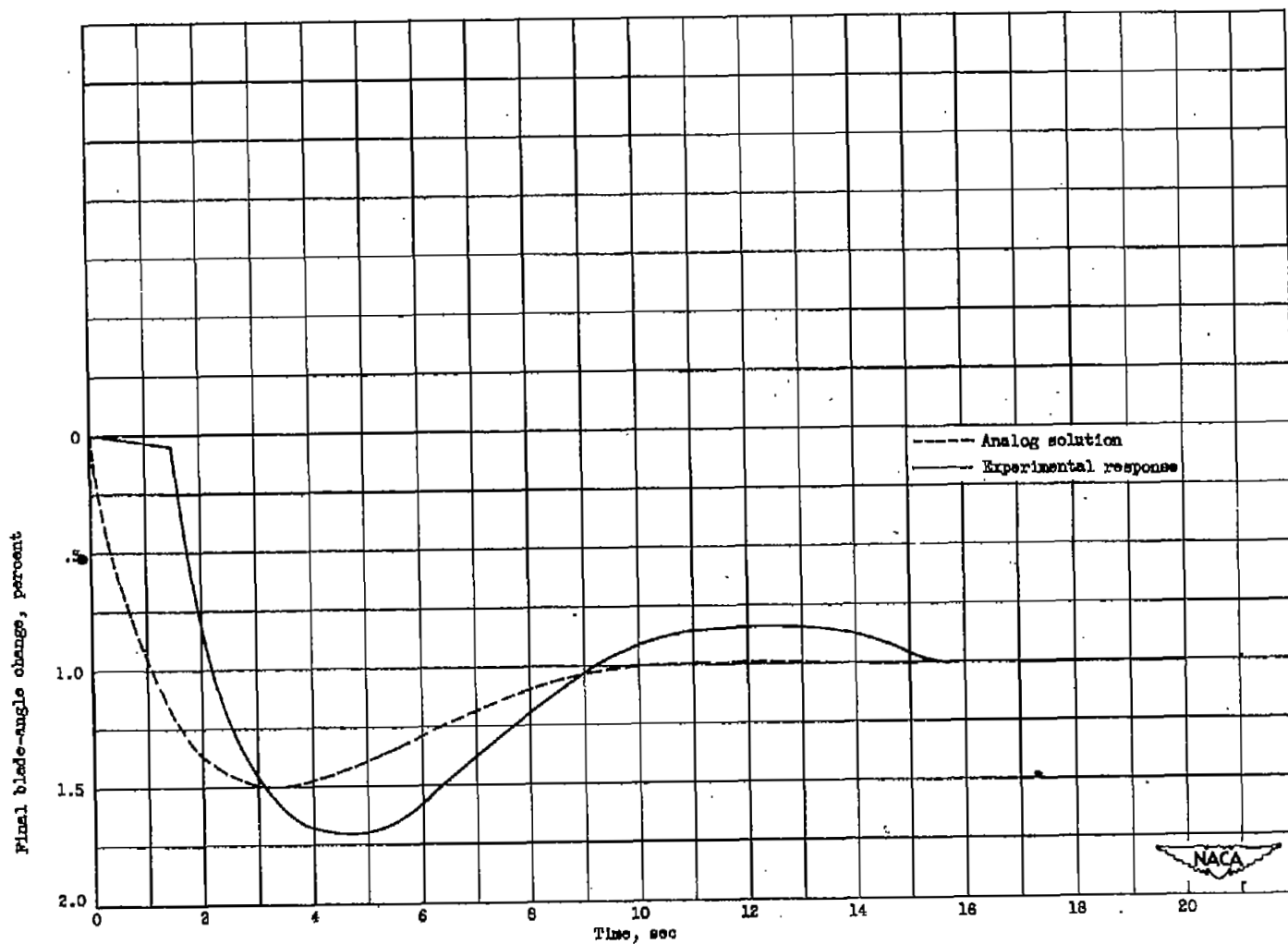
(d) Blade angle. K_p, 0.0040 deg β/rpm; K_I, 0.0032 (deg β/sec)/rpm; τ_c, 1.25 sec; turbine-speed change, 11,440 to 12,080 rpm; blade-angle change, 28.4° to 23.4°; load-torque change, 333 to 279 foot-pounds.

Figure 6. - Concluded. Comparison of experimental transient response and analog solutions to ramp-type disturbances in speed setting with constant fuel flow for turbine-propeller engine and turbine-speed - blade-angle control system. (Analog solution determined from harmonic analysis and transfer function approximation.)
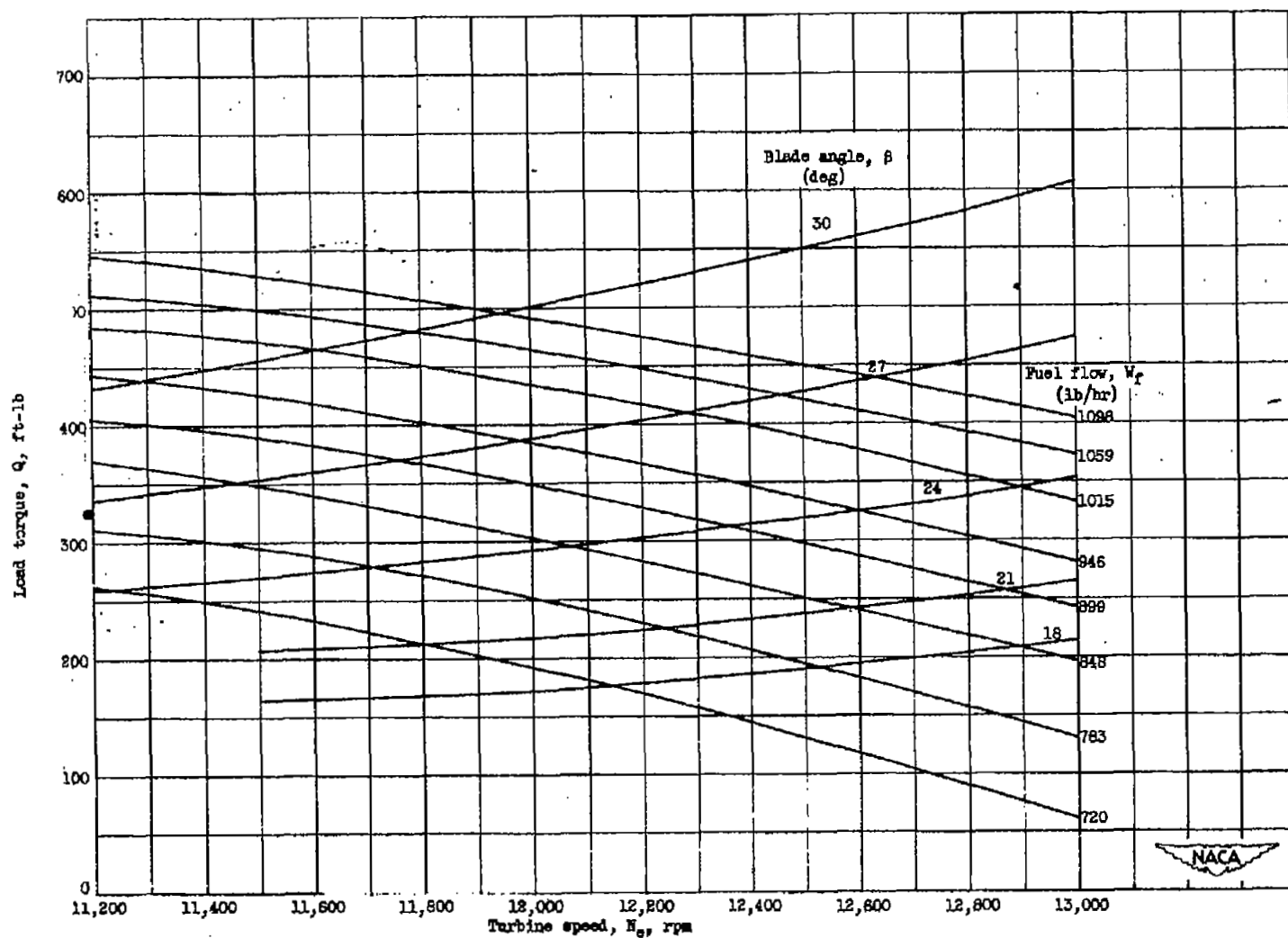
Figure 7. - Relation between engine load torque and turbine speed for constant blade angle and fuel flow as obtained from sea-level zero-ram experimental data for turbine-propeller engine with Aeroproducts A542F-17 propeller.

Altitude (ft)	K_p $\left(\dfrac{\deg \beta}{rpm}\right)$	K_i $\left(\dfrac{\deg \beta/sec}{rpm}\right)$	K_θ $\left(\dfrac{rpm}{\deg \beta}\right)$	K_β $\left(\dfrac{\deg \beta}{\deg \beta}\right)$	τ_β (sec)	τ_θ (sec)	τ_r (sec)	τ_c (sec)
—— Sea level	0.0084	0.0068	226	1	0.3	2.9	0.3	1.23
----- 25,000	.0084	.0068	205	1	.3	7.1	.3	1.23
—·— 35,000	.0084	.0068	197	1	.3	10.8	.3	1.23
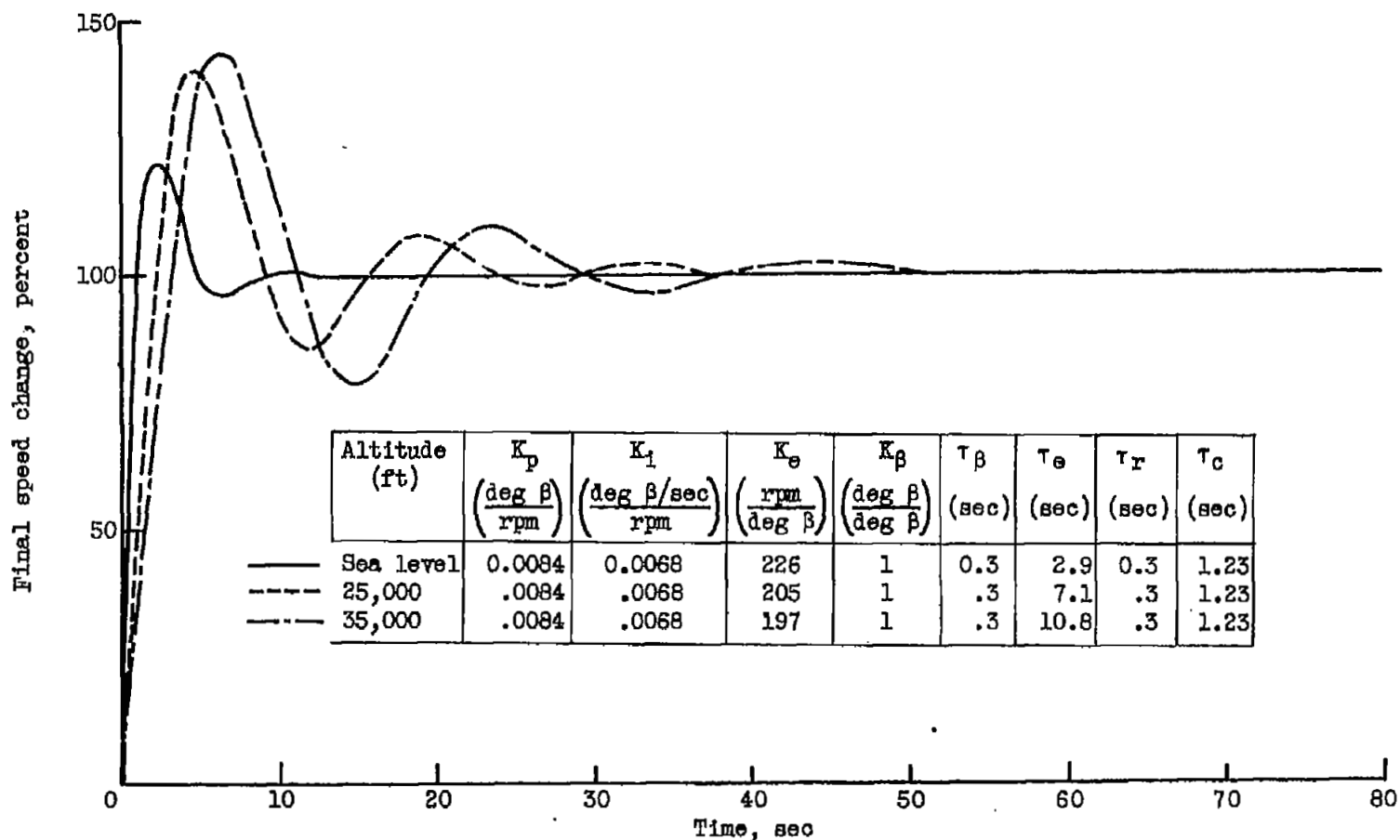
(a) Turbine speed.

Figure 8. - Computed altitude transient response of turbine speed and blade angle for turbine-propeller engine and turbine-speed - blade-angle control system with fixed-control constants.
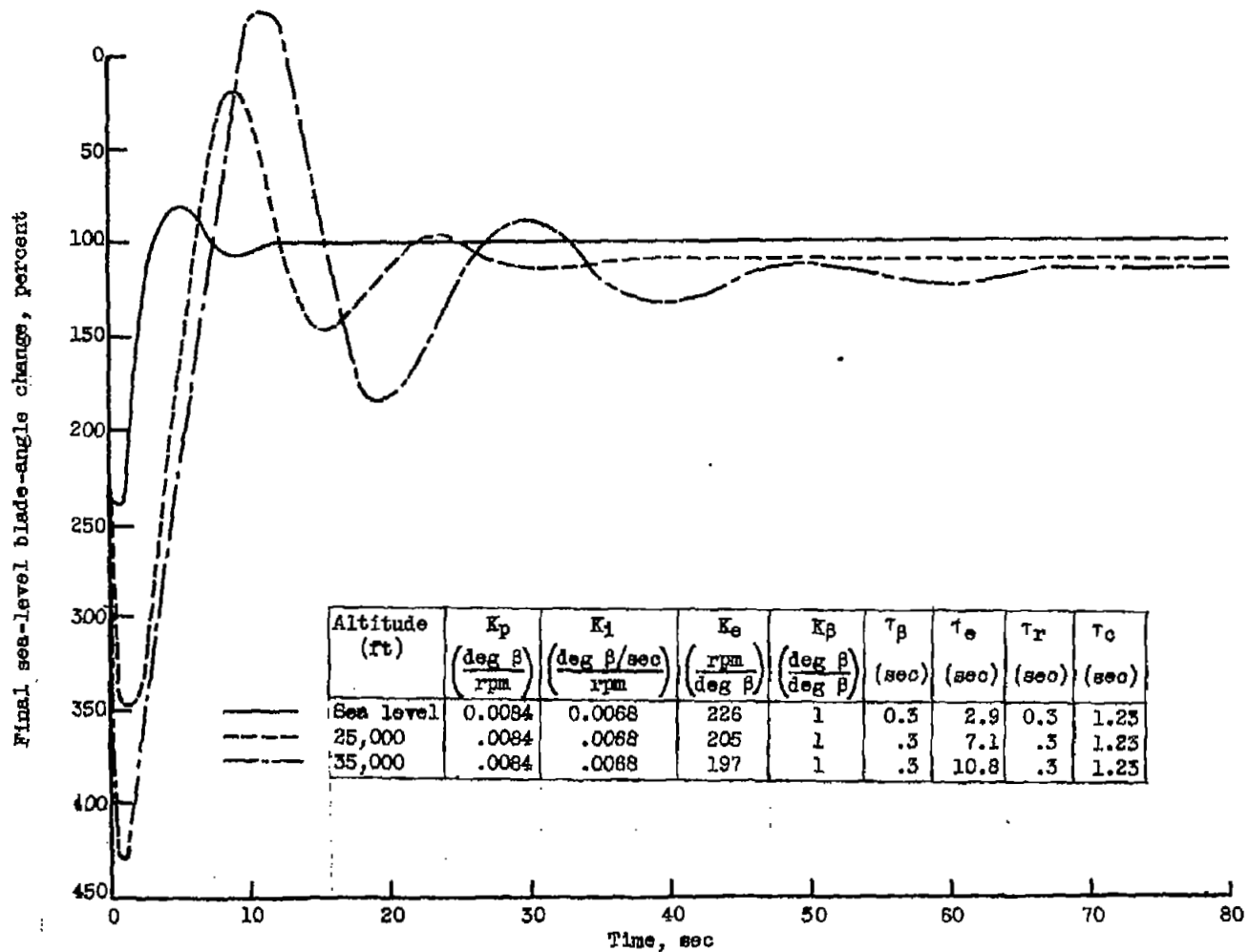
(b) Blade angle.

Figure 8. - Concluded. Computed altitude transient response of turbine speed and blade angle for turbine-propeller engine and turbine-speed - blade-angle control system with fixed-control constants.

Sea-level response.

Control constants varied to maintain sea-level turbine-speed response at 35,000 ft.

Control constants varied to maintain sea-level loop gain and ratio of engine time constant to control time constant at 35,000 ft.

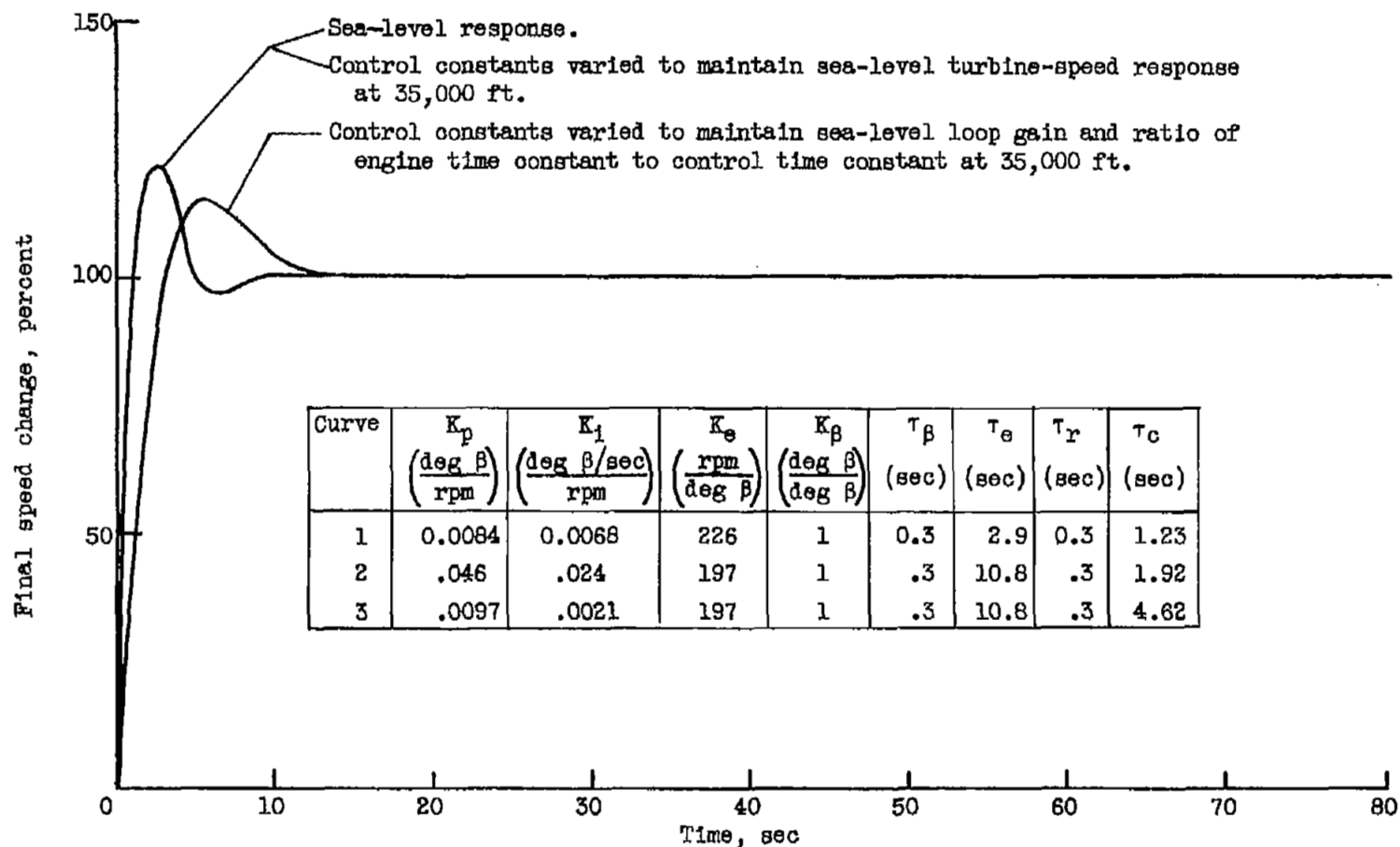| Curve	K_p $\left(\dfrac{\deg \beta}{\text{rpm}}\right)$	K_i $\left(\dfrac{\deg \beta/\text{sec}}{\text{rpm}}\right)$	K_e $\left(\dfrac{\text{rpm}}{\deg \beta}\right)$	K_β $\left(\dfrac{\deg \beta}{\deg \beta}\right)$	τ_β (sec)	τ_e (sec)	τ_r (sec)	τ_c (sec)
1	0.0084	0.0068	226	1	0.3	2.9	0.3	1.23
2	.046	.024	197	1	.3	10.8	.3	1.92
3	.0097	.0021	197	1	.3	10.8	.3	4.62

(a) Turbine speed.

Figure 9. - Computed turbine speed and blade angle transient response at sea level and 35,000 feet of turbine-propeller engine with turbine-speed - blade-angle control system for various values of control constants.

Curve	K_p $\left(\dfrac{\deg\ \beta}{\text{rpm}}\right)$	K_1 $\left(\dfrac{\deg\ \beta/\text{sec}}{\text{rpm}}\right)$	K_e $\left(\dfrac{\text{rpm}}{\deg\ \beta}\right)$	K_β $\left(\dfrac{\deg\ \beta}{\deg\ \beta}\right)$	τ_β (sec)	τ_e (sec)	τ_r (sec)	τ_c (sec)
1	0.0084	0.0068	226	1	0.3	2.9	0.3	1.23
2	.046	.024	197	1	.3	10.8	.3	1.92
3	.0097	.0021	197	1	.3	10.8	.3	4.62

Sea-level response.

Control constants varied to maintain sea-level turbine-speed response at 35,000 ft.

Control constants varied to maintain sea-level loop gain and ratio of engine time constant to control time constant at 35,000 ft.
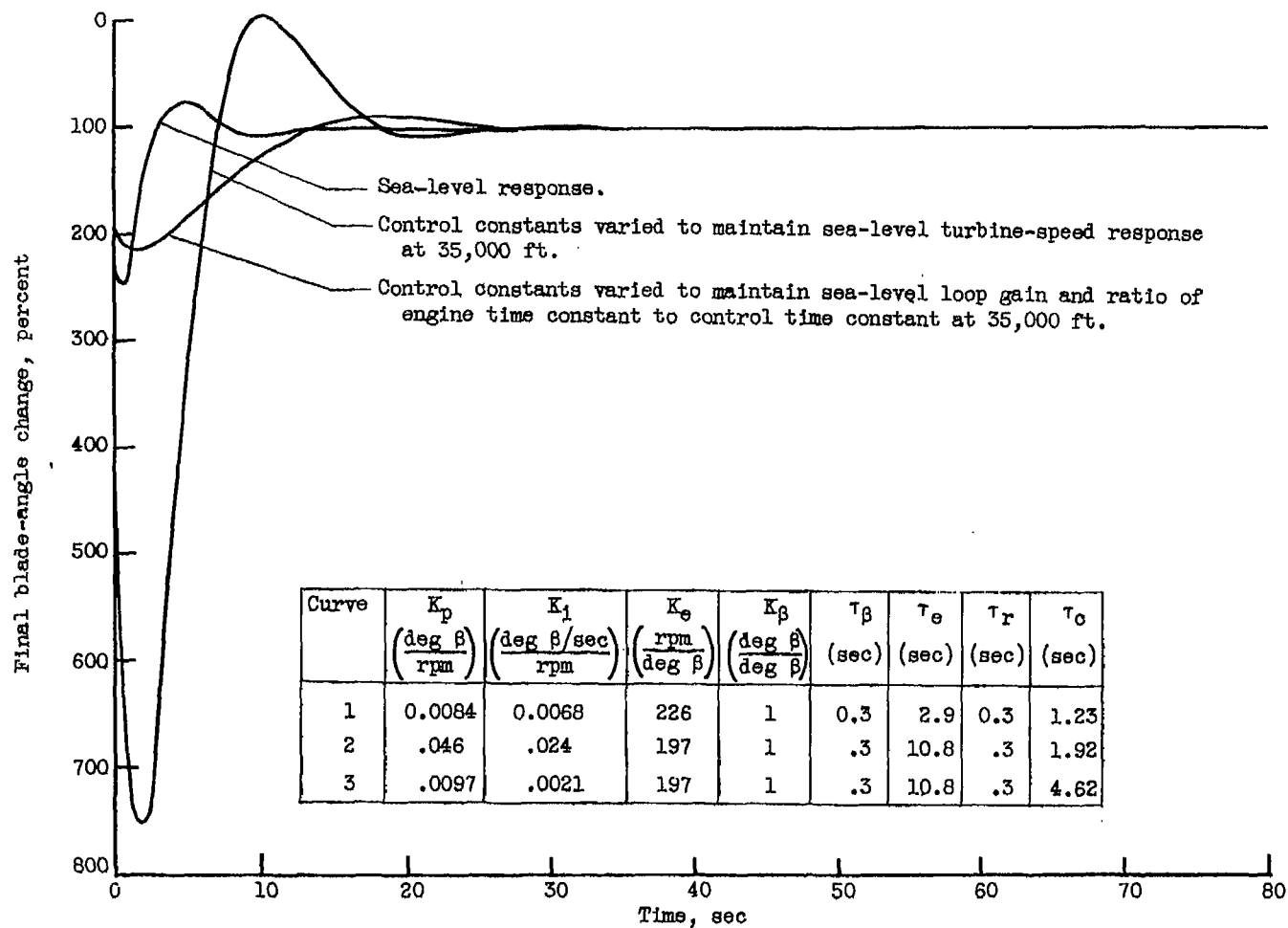
(b) Blade angle.

Figure 9. - Concluded. Computed turbine speed and blade angle transient response at sea level and 35,000 feet of turbine-propeller engine with turbine-speed - blade-angle control system for various values of control constants.